Physics – Uspekhi **42** (11) 1121 – 1138 (1999)

REVIEWS OF TOPICAL PROBLEMS PACS numbers: **64.30.+t**, **71.20.–b**, **71.30.+h**, **74.25.–q**

Hydrogen at high pressure

E G Maksimov, Yu I Shilov

Contents

Abstract. Experimental and theoretical work on solid hydrogen under high pressure is reviewed with special emphasis on three aspects of the field. The first concerns the equation of state of hydrogen and the properties of its molecular phase. Both experimental and theoretical studies show that hydrogen has a rich variety of unusual properties even in its molecular phase, as the formation of many highly anisotropic crystal structures with little energy difference exemplifies. The second aspect is the insulator-metal transition which, while customarily associated with atomization, i.e., with the dissociation of hydrogen molecules, is also possible in the molecular phase according to recent theoretical studies. In discussing the metallic phase, finally, the existence of a metastable phase at normal pressure and prospects for the high superconducting transition temperatures in metallic hydrogen are considered.

1. Introduction

Theoretical studies of crystalline hydrogen properties as a function of pressure have been in progress for more than half a century, beginning from the classic study by Wigner and Huntington [1]. In that work it was predicted for the first time that hydrogen that crystallizes under low pressures in a molecular insulating phase should transform to a monoatomic metallic phase under higher pressures. The transition pressure predicted in that work turned out to be rather low, $p_c = 25$ GPa. The obvious simplicity of this system was one of the motives for the theoretical study of crystalline hydrogen. Actually, a hydrogen atom is the simplest quantum system and, in addition, an exactly solvable one. A hydrogen molecule that is also the simplest of possible molecules contains only two electrons, and hence it may be a good candidate to be investigated using various approximate methods of quantum-mechanical calculations. However, it turned out before long that this simplicity is only seeming. Thus, further calculations of p_c [2 – 4] lead to a spread in the values over the range 25 to 1500 GPa, that is from 250 kbar to 15 Mbar (1 bar $= 10^5$ Pa, 1 atm $= 1.01325 \times 10^5$ Pa).

As is evident from recent experimental and theoretical work done in the late 80s – early 90s (see, for example, the review [5]), even in its molecular phase, high-pressure crystalline hydrogen exhibits a number of properties rather unusual among molecular crystals. Moreover, its behavior is difficult to explain unambiguously by theory.

Another important motive for the study of crystalline hydrogen is related to the predictions [6 – 8] which appeared in the 70s of very interesting, even exotic, phenomena, which may exist in the hydrogen metallic phase. Thus, it was assumed [6] that high-temperature superconductivity with a critical temperature $T_c \sim 200$ K should occur in the metallic phase of hydrogen. Such a high value of T_c is basically due to the high Debye temperature of hydrogen caused by its small atomic mass, ($\Theta_D \sim M^{-1/2}$). It was assumed that even more exotic possibilities might be realized in the metallic phase. For example, it was discussed [7] that a liquid phase of metallic hydrogen might be stabilized with zero-point motion (ZPM) at sufficiently low temperatures, by analogy with liquid helium. In such a situation, with a two-component Fermi-liquid (protons and electrons for hydrogen), or a mixture of Fermi- and Bose-liquids (for deuterium), either the superconductivity of both Fermi-liquids (for H) or superconductivity of electrons and superfluidity of the Bose-liquid (for D) is possible, correspondingly. Notice that it is all these interesting properties possibly exhibited by high-density hydrogen which encouraged Vitaly Ginzburg to inscribe the study of hydrogen in his well known 'list of the key problems in physics' (to this day, the problem of hydrogen still remains in the list) [9].

A nontrivial idea of primary interest concerning the properties of the hydrogen metallic phase has been advanced by Yury Kagan and his group [8]. Their calculation made within the perturbation theory in the electron-proton poten-

E G Maksimov P N Lebedev Physics Institute,
Russian Academy of Sciences
Leninskiĭ prosp. 53, 117924 Moscow, Russian Federation
Tel. (7-095) 135 75 11. Fax (7-095) 135 85 33
E-mail: maksimov@lpi.ru
Yu I Shilov Russian Federal Nuclear Center — All-Russian Research Institute of Experimental Physics
Prosp. Mira 37, 607190 Sarov, Nizhniĭ-Novgorod Region,
Russian Federation
Tel. (7-83130) 569 74. Fax (7-83130) 545 65
E-mail: otd4@expd.vniief.ru

Received 14 September 1999
Uspekhi Fizicheskikh Nauk **169** (11) 1223 – 1242 (1999)
Translated by E G Maksimov; edited by M V Magnitskaya

tial demonstrated that a metastable metallic phase of hydrogen might exist at zero pressure. The mere fact of the existence of metastable phases is not contrary to the common laws of nature. An important point is that the lifetimes of such phases should be long enough to measure their characteristics and, possibly, even to find where such phases might be used. At least one example is familiar to everybody — the existence of a metastable phase of carbon at zero pressure. This phase is diamond. But, graphite is a stable phase of carbon at $p = 0$. It is well known also that the lifetime of metastable diamond is certainly enough to examine its properties and to use it in practice.

The possible existence of a metastable phase in metallic hydrogen at $p = 0$ has been a subject of animated discussion [10, 11]. Considerations have been advanced to challenge such a possibility, but actually, this problem still remains unsolved. Beginning in the 70s, and especially in recent years, a large body of experimental work on hydrogen has been done at high pressure (see the review [5] and references therein). These measurements were carried out both at static compression, typically with the use of diamond-anvil cells, and at dynamic compression, by means of various explosion methods. Even on static compression in diamond-anvil cells, pressures of the order of 300 GPa were achieved [12] which corresponds to a twelve-fold solid compression of crystalline hydrogen. Most of the theoretical estimates indicated that hydrogen would become a metal at such pressures. It is most likely, however, that the insulator-metal transition has not been observed experimentally in the accessible range of pressures. It was stated [13, 14] that the metallization of hydrogen on compression was observed by means of explosion techniques. Here, however, the problem of crucial importance that is incompletely understood are the temperature values occurring in the experiment. Related to this problem is the question of whether or not the reported insulator-metal transition is due to the direct effect of high temperatures which occur in the system in the course of shock-wave compression experiment.

This review is devoted to the presentation and discussion of most problems touched upon above.

2. The properties of molecular hydrogen at high compression

Molecular crystalline hydrogen has a variety of peculiar properties responsible for its dissimilarity to other molecular crystals. The main distinction is, perhaps, that the rotation of molecules is not suppressed at low pressures, even in the crystalline state. Because of the coupling between nuclear spins and rotational states of the molecules with a given moment J, two modifications of hydrogen molecules are available — para- and ortho-hydrogen — with even or odd J values, correspondingly. At zero temperature $T = 0$, the concentration ratio $c_{\text{ortho}} : c_{\text{para}} = 0$. Because of a small difference in energy between ortho- and para-states ($\Delta E \approx 170.5$ K), the concentration ratio increases to 3:1 as the temperature is increased to room temperature. Ortho-hydrogen possesses an electric quadrupole moment, and this may lead to a number of essential effects in the crystal at low pressures. In particular, quadrupole ordering occurs in pure ortho-hydrogen at $T \approx 3-4$ K. Properties of molecular hydrogen at low pressure are described comprehensively in the review [15], and in what follows we shall not touch upon this problem.

The equation of state (EOS), i.e. the relation between pressure and volume $p = p(V)$, of molecular hydrogen has long been investigated both theoretically and experimentally. One of the important motives of this work is that the Sun and giant planets — Jupiter and Saturn — are more than 90% hydrogen. A major part of this work pursued astrophysical objectives [16]. Earlier investigations of the EOS are reviewed in Ref. [17]. Recently, considerable advances have been made in the field of experimental research, through the use of the diamond-cell technique. In Ref. [18] the EOS of deuterium was measured to 32 GPa by means of neutron diffraction. The use of the deuterium in this work is due to the fact that its cross-section of coherent neutron scattering is three times as large as in hydrogen. The crystal structure of deuterium was also determined. The hexagonal-close-packed (hcp) structure was observed to exist over the whole range of pressures measured, the c/a ratio decreasing continuously from 1.634 at $p = 0$ to 1.62 at $p \approx 32$ GPa. In Ref. [18] is reported that an error of pressure determination did not exceed a value of $\pm(0.07-0.1)$ GPa.

Further experimental study of the EOS for hydrogen was made by a research group from the Carnegie Institution, Washington, first to the pressure of 42 GPa [19] and then to 120 GPa [20]. In these experiments the X-ray diffraction in crystalline hydrogen compressed using a diamond-anvil cell was investigated. In the course of work the investigators had to overcome severe difficulties related to hydrogen's small X-ray-scattering efficiency and to a considerable reduction in the diamond-cell volume needed to achieve high pressures. Highly intensive synchrotron radiation was used as the X-ray source. A new experimental technique was developed on the basis of a combination of standard single-crystal X-ray methods with energy-dispersive diffraction [21]. The investigators estimate the accuracy of the pressure measurement as $\Delta p = \pm 0.3$ GPa and that of the volume measurement as $\pm 2 \times 10^{-3}$ cm^3 mole^{-1}.

The solid line in Fig. 1 represents the EOS of hydrogen obtained by the Carnegie Institution group. The investigators adjusted a Vinet equation [22] to describe their experimental

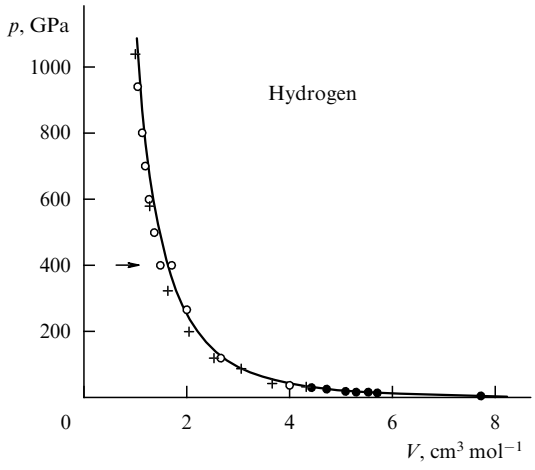

Figure 1. Equation of state of solid hydrogen: neutron diffraction at static compression [18] (•); shock compression [13, 23] (○); static X-ray data fitted in [5] using the Vinet equation (solid line); first-principles calculations [26] using the equations (1), (5) (+). The arrow indicates a possible phase transition with an 8% increase in density obtained in [13, 23] by processing of shock compression data.

data to 120 GPa. The main thing we would like to emphasize concerning this picture is the surprisingly good agreement of the new data of the EOS of molecular hydrogen with the shock-compression results obtained more than 20 years ago by Kormer's group [13, 23] from the All-Russian Research Institute of Experimental Physics (VNIIEF, at that time Arzamas-16). The results obtained by the VNIIEF group in the pressure range from about 40 to 400 GPa match with good accuracy the curve that represents both the Vinet equation and the data to 120 GPa obtained by the Carnegie Institution team. An extra point at 400 GPa, as well as the whole EOS curve, was obtained by the VNIIEF group [23] by means of calculations. This point indicates the occurrence at $p \approx 400$ GPa of a phase transition with an increase in density by $\approx 8\%$.

The Birch equation [24] and Murnaghan equation [25] are frequently used in high pressure physics to describe EOS. The Birch equation was derived in the framework of the elastic deformation theory to second order in such deformations. It has the following form:

$$p(X) = 1.5K_0(X^{-7/3} - X^{-5/3})\left[1 - \xi(X^{-2/3} - 1)\right]. \qquad (1)$$

Here $X = V/V_0$, V_0 is the equilibrium volume at $p = 0$, K_0 is the bulk modulus, and is

$$\xi = 3 - \frac{3}{4}\frac{\partial K_0}{\partial p}. \qquad (2)$$

The Murnaghan equation can be derived from Eqn (1) assuming that the bulk modulus K_0 depends linearly on pressure:

$$K_0(X) = K_0 + K_0' p(X), \qquad (3)$$

$$K_0' = \frac{\partial K_0}{\partial p}. \qquad (4)$$

It has the form

$$p(X) = \frac{K_0}{K_0'}\left[\left(p_0\frac{K_0'}{K_0} + 1\right)X^{-K_0'} - 1\right], \qquad (5)$$

where p_0 denotes $p(X = 1)$.

Strictly speaking, i.e. with the use of experimental data on bulk modulus K_0 and its pressure derivative K_0', the Birch and Murnaghan equations are applicable only over a very limited range of compressions and cannot be employed for representing the EOS of hydrogen to pressures of 120 GPa which correspond to an almost ten-fold reduction in specific volume. Nevertheless, in a number of cases the EOS can be reasonably well fitted with Eqns (1) and (5), by using the values of K_0 and K_0' as adjustable parameters. It is this technique that is applied in Ref. [26] for representing the EOS determined from so-called *ab initio* calculations at several volumes.

Most theoretical attempts to find the EOS of molecular hydrogen are based on various approximate expressions for the intermolecular interaction. Since hydrogen molecules have an almost spherical distribution of the electron charge as well as a small size, their behavior is similar to that of noble gas molecules in many cases. The first calculation of an EOS for the hydrogen molecular phase was performed by Trubitsyn [27] who used an intermolecular potential in a simple analytical form of van der Waals attraction combined with short-range repulsion. He determined the free parameters of the potential by adjusting to experimental data on the EOS to 20 GPa available at that time. Subsequently, Ross [3] attempted to determine the EOS for hydrogen more accurately to 100 GPa using the data of shock compression experiments. He applied the same analytical expression for intermolecular potential as Trubitsyn did. Phenomenological intermolecular potentials were compared [28] with potentials obtained from *ab initio* calculations based on the quantum-mechanical consideration of two and four hydrogen molecules. The important role of many-body interactions was emphasized. In Ref. [29] three-particle interactions were consistently included in calculation of the EOS for molecular hydrogen. Actually, as became clear from the measurements of EOS to 120 GPa, all the previous attempts to construct the EOS using various intermolecular potentials led to a 'harder' EOS than observed experimentally.

In this respect, the following proposal advanced in Ref. [22] seems to be quite interesting: to write a universal EOS for any kind of solid on the basis of an approach just opposite to that of the works discussed above. While the authors of Refs [3, 27–29] used the idea of molecular hydrogen as a system with almost non-overlapping electron shells of different molecules and with a given intermolecular interaction, in Ref. [22] it was assumed that the EOS for molecular and ionic crystals, along with covalent semiconductors is mainly determined by effects related to the electron-shell overlap. Previously, an appropriate EOS was written for metals [30], where the electron subsystem with strongly overlapping shells makes, actually, the basic contribution to the EOS. This EOS has the following form:

$$p(X) = 3K_0X^{-2/3}\left(1 - X^{1/3}\right)\exp\left[\frac{3}{2}(K_0' - 1)\left(1 - X^{1/3}\right)\right]. \qquad (6)$$

It was shown [22] that expression (6), commonly referred to as the Vinet equation, described quite well the then available experimental data of the EOS for molecular hydrogen to 25 GPa. In Ref. [22] the experimental values of K_0, K_0' and V_0 were used. Subsequently, equation (6) was applied [19] to represent experimental results to 42 GPa. In this case an experimental value of V_0 equal to 25.433 $cm^3\,mole^{-1}$ was taken, while the values of K_0 and K_0' were used as adjustable parameters. It was obtained that $K_0 = 0.162$ GPa and $K_0' = 6.813$ GPa which is not too different from experimental data at $p = 0$.

Besides semi-phenomenological [3, 27–29] and purely phenomenological [22] approaches to the EOS calculation for molecular hydrogen, a serious effort was made to calculate the EOS *ab initio* [26, 31–34]. In Refs [26, 31] a method of total energy calculation based on the density functional theory (DFT) [35] was used which is standard in state-of-the-art solid state physics. In those calculations, the protons were treated as classical particles rigidly fixed to the sites of an appropriate crystal lattice. In Ref. [31] phonon spectra in several symmetrical directions were calculated and then used to find the zero-point contribution of lattice to the total energy and pressure. The contribution turned out to be much larger than in many other molecular crystals. This is directly related to the smallness of proton mass and points out the important role possibly played by quantum effects in the behavior of proton lattice. In Ref. [32, 33] quantum Monte Carlo methods were applied to calculate the EOS of

hydrogen, both electrons and protons being treated as quantum particles. A detailed comparison [20] of band structure calculations with experimental data of EOS to 120 GPa demonstrated that the calculated specific volume is underestimated at low pressures ($p < 100$ GPa) and overestimated at higher p by $\approx 6\%$ on average, a deviation in compressibility being even greater. In Monte Carlo simulations the specific volume is overestimated by $\approx 8\%$ as compared to the experimental data. Thus, the available *ab initio* methods do not provide the accuracy required for calculating the EOS of high-pressure crystalline hydrogen. We shall return in this review to the discussion of possible reasons for such a situation. For completeness sake, one should mention a recent quantum Monte Carlo simulation [34] where the EOS of molecular hydrogen was found to practically coincide with the experimental data. Nevertheless, these results cannot be regarded as a considerable advance in the field of theoretical study of compressed hydrogen since phenomenological pair potentials of the proton-proton interaction with adjustable parameters were used in Ref. [34].

In addition to the EOS, the $p-T$ phase diagram of hydrogen was studied basically by the effort of two research groups in the USA [36–38]. It is schematically plotted in Fig. 2. The phase diagrams of both isotopes, H_2 and D_2, are much alike, they are different only in the position of boundary between the phases I and II. As is seen in Fig. 2, at least three different phases of crystalline hydrogen exist in the pressure range to ~ 200 GPa. Experimentally, except for phase I, little is known about these phases and the character of transitions between them. Only that all three phases apply to the molecular hydrogen solid may be thought of as well-founded experimentally [36]. In the experiments, all the boundaries between phases were detected through the changes in various vibration modes of corresponding crystal lattices (see the review [5] for more detail). Characteristic of the transition from phase I to phase II is that the optically active modes lacking in phase I appear in the vibration spectrum of the phase II [37, 38]. The transition from phase II to phase III is marked by discontinuous changes in both IR and Raman modes. Another distinctive feature of phase III is a sharp increase in the oscillator strengths of optically active modes [36].

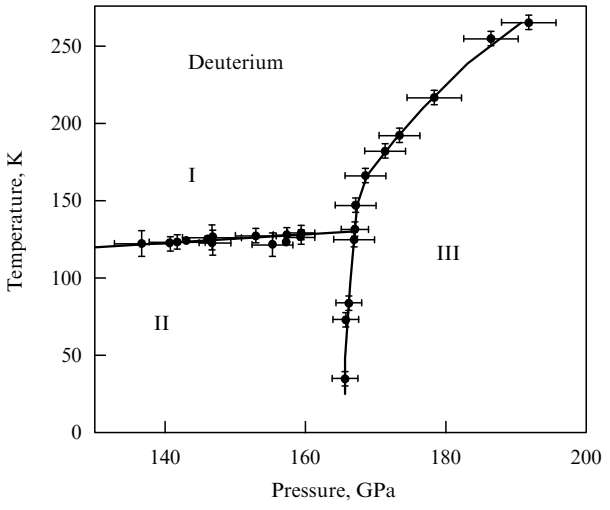

Figure 2. Megabar-pressure phase diagram of deuterium. The solid circles with error bars correspond to Raman and infrared measurements [36].

The crystal structure of phase I is reliably established by means of both neutron [18] and X-ray [19] measurements. In this phase the centres of H_2 molecules form the hcp structure, while the molecules themselves rotate freely owing to the occurrence of both thermal and zero-point librons (rotational modes). Because of the almost spherical distribution of electron density in hydrogen molecules there are no optically active modes in this phase, and the infrared absorption occurs only through second-order processes. A wide absorption band appears around ≈ 4500 cm^{-1} that is the energy of intramolecular vibron. The very fact that optically active modes arise in phase II is, first of all, evidence of molecular ordering occurring in this phase and it allows the exclusion of at least some possible ways of such ordering. However, the nature of the ordering in question remains to be understood. Thus, a model was proposed [39] of quantum orientational ordering of hydrogen molecules in phase II. It was assumed that in phase II the hydrogen molecules remain freely rotating with rather high angular momenta $J = 2, 4$, but at the I–II boundary the ordering of quantization axes of molecular rotation takes place. Then, according to Ref. [39] a classical ordering of molecular axes occurs at the boundary of phases II and III. In most other theoretical studies on this problem [34, 40, 41] the phase boundaries I–II and II–III are associated with a different type of ordering of both the molecular axes and molecular centres. Since the thermal librons as well as the zero-point ones necessarily exist in systems with an ordering of molecular axes, then it is absolutely unclear whether there is any principal difference between the quantum ordering of quantization axes and the classical ordering of molecular axes. It is quite possible that nothing more than a proper inclusion of the libron-mode influence on the properties of systems with ordering of molecular axes is needed. At the moment, this question is quite difficult to answer because a detailed analysis of the quantum-ordered phase properties is absent in Ref. [39].

A large body of theoretical work [39–48] is available on the structure of high-pressure molecular hydrogen. In these investigations, two of above-mentioned *ab initio* methods for calculating the crystal properties are basically employed. This is the density functional method of electron-band structure calculation [38, 39, 41–44] and the quantum Monte Carlo method [34, 47, 48]. In Refs [40, 46] a method of *ab initio* molecular dynamics (AIMD) was used. Before discussing these studies in detail, we would like to formulate what follows from them. To start with, a variety of crystal structures of nearly the same energy are predicted for molecular hydrogen at high pressure. In this regard the EOS depends only weakly on the type of crystal structure stable at a given pressure, but many other properties of such a system may crucially depend on its crystal structure. In the high-pressure region, anisotropic and very complex structures with many molecules per unit cell have the lowest energy, at least prior to a transition to a monoatomic phase. Most of these structures can be derived from an hcp lattice characteristic of phase I by changing the ordering of the molecular axes and by slightly displacing the molecular centres off positions corresponding to the regular hcp structure.

Below we shall describe in brief the methods of *ab initio* calculations. As noted already, most of them are based on the density functional theory. The essence of this theory is as follows. It is proven that the ground-state energy of a system of interacting electrons E_{el} in an external field (here in the field of protons) is a single-valued functional of the electron

density. The real distribution of electron density is determined by minimizing this functional:

$$\frac{\delta E_{\rm el}\{\rho(\mathbf{r})\}}{\delta\rho(\mathbf{r})} = 0\,. \tag{7}$$

The energy $E_{\rm el}\{\rho(\mathbf{r})\}$ can be presented in the form

$$E_{\rm el}\{\rho(\mathbf{r})\} = T_0\{\rho(\mathbf{r})\} + \frac{e^2}{2}\int\frac{\rho(\mathbf{r})\rho(\mathbf{r}')}{|\mathbf{r}-\mathbf{r}'|}\,\mathrm{d}\mathbf{r}' + \int\rho(\mathbf{r})V_{\rm ext}(\mathbf{r})\,\mathrm{d}\mathbf{r} + E_{\rm xc}\{\rho(\mathbf{r})\}\,. \tag{8}$$

Here $T_0\{\rho(\mathbf{r})\}$ is the kinetic energy of a system of noninteracting electrons with the same density as that of the crystalline system under consideration; $V_{\rm ext}(\mathbf{r})$ is an external potential. In case of crystal it is nothing but a sum of potentials of nuclei (protons):

$$V_{\rm ext}(\mathbf{r}) = \sum_n V_n(\mathbf{r}-\mathbf{R}_n)\,. \tag{9}$$

The functional of exchange-correlation energy is denoted as $E_{\rm xc}\{\rho(\mathbf{r})\}$. At present, the exact form of this functional is unknown. In most calculations the so-called local density approximation is used. It means that $E_{\rm xc}\{\rho(\mathbf{r})\}$ is presented in the form

$$E_{\rm xc}\{\rho(\mathbf{r})\} = \int\rho(\mathbf{r})\varepsilon_{\rm xc}\{\rho(\mathbf{r})\}\,\mathrm{d}\mathbf{r}\,, \tag{10}$$

where an expression obtained for the homogeneous electron gas with a given density is used for $\varepsilon_{\rm xc}\{\rho(\mathbf{r})\}$. This expression for $\varepsilon_{\rm xc}\{\rho(\mathbf{r})\}$ is well known. Then, with $\rho(\mathbf{r})$ written as the density of a system of non-interacting electrons in an external self-consistent field

$$\rho(\mathbf{r}) = \sum_i^{\varepsilon_m}|\psi_i(\mathbf{r})|^2\,, \tag{11}$$

one can get a Kohn–Sham equation [35] for wave functions $\psi_i(\mathbf{r})$:

$$\left[-\frac{\nabla^2}{2m} + V_{\rm eff}(\mathbf{r})\right]\psi_i(\mathbf{r}) = \varepsilon_i\psi_i(\mathbf{r})\,, \tag{12}$$

where the effective potential $V_{\rm eff}(\mathbf{r})$ has the form

$$V_{\rm eff}(\mathbf{r}) = \sum_n V_n(\mathbf{r}-\mathbf{R}_n) + e^2\int\frac{\rho(\mathbf{r}')}{|\mathbf{r}-\mathbf{r}'|}\,\mathrm{d}\mathbf{r}' + V_{\rm xc}\{\rho(\mathbf{r})\}\,, \tag{13}$$

$$V_{\rm xc}\{\rho(\mathbf{r})\} = \frac{\delta E_{\rm xc}\{\rho(\mathbf{r})\}}{\delta\rho(\mathbf{r})}\,. \tag{14}$$

Within the local density approximation for $E_{\rm xc}\{\rho(\mathbf{r})\}$ (10) all the quantities in Eqns (8)–(14) are well defined, and the calculation of the ground-state energy of the electron subsystem can be carried through.

Formally, the procedure of further calculations is rather simple. In the initial stage a crystalline electron density is constructed, for example, following Mattheiss, i.e. as a superposition of atomic electron densities. It is substituted into expression (13) for the effective potential. Then, the Kohn–Sham equation (12) is solved and a new density is defined from its solution by formula (11). After that a new potential $V_{\rm eff}(\mathbf{r})$ is constructed using the new density, and the equation of Kohn–Sham is solved again. The whole cycle is iterated to self-consistency. As a result, the ground-state energy $E_{\rm el}$ of electrons is calculated by formula (8) using the solutions obtained to the Kohn–Sham equation. To calculate the total energy of the crystal, the Coulomb energy of nuclei (protons) is added to $E_{\rm el}$:

$$E = E_{\rm el} + \frac{e^2}{2}\sum_{n,n'}\frac{1}{|\mathbf{R}_n-\mathbf{R}_{n'}|}\,. \tag{15}$$

All these calculations can be performed for any crystalline structure and for any interatomic spacing allowing us to get the equation of state and to find a lattice corresponding to the global energy minimum.

In fact, the above calculational procedure is quite complicated and tedious. This is easy to understand even from the fact that the very procedure of solving the Kohn–Sham equation with a periodic potential and the calculation of corresponding Bloch functions $\psi_{\mathbf{k}\lambda}(\mathbf{r})$ ($\mathbf{k}$ is the electron momentum, λ is the number of energy band) is a large separate chapter of solid state theory [49]. Naturally, we cannot discuss here in detail all the problems related to the practical realization of the procedure of band structure calculation, thus, we consider briefly the possible causes of different-type errors occurring in the scheme described. There are a few such causes. First of all, this is the local density approximation for exchange-correlation energy. The electron density distribution in crystalline hydrogen is far from the homogeneous one for which this approximation is exact. In some investigations of hydrogen (for example, Refs [40, 42]) attempts were made to go beyond this approximation, however, this problem has not been seriously studied with respect to the calculation of crystalline hydrogen. The second cause that now is specific just to hydrogen is that in band structure calculations the protons are treated as classical particles rigidly fixed to the sites of a particular lattice [39–45]. There is great evidence, however, that quantum fluctuations of the protons are of great importance for crystalline hydrogen, and hence the ZPM must be taken into account, even at $T = 0$.

The first attempt to include the influence of proton ZPM on the properties of high-density hydrogen was made in Ref. [50] in calculating the metallic phase. The total energy of the crystal was written in terms of perturbation theory in electron-proton interaction:

$$E = \frac{1}{2}\sum_{\mathbf{q},\lambda}\hbar\omega(\mathbf{q},\lambda) + \sum_{\mathbf{R}\neq 0}U(\mathbf{R}) + \text{ structure-independent.} \tag{16}$$

Here the first sum is taken over phonon frequencies. Taking into account that the amplitude of proton ZPM is rather large and hence anharmonism is essential, the phonon frequency calculation [50] was performed using the quasiharmonic approximation. In this approximation the phonon frequencies are determined by solving a standard eigenvalue equation:

$$M\omega^2(\mathbf{q},\lambda)e_\alpha(\mathbf{q},\lambda) = e_\beta(\mathbf{q},\lambda)\frac{1}{N}\sum_{\mathbf{R}\neq 0}\left\{(\cos\mathbf{qR}-1) \times\int\frac{4\pi e^2}{k^2\varepsilon(\mathbf{k})}\,k_\alpha k_\beta\exp\left[-\frac{1}{2}\,k_\mu k_\nu\lambda_{\mu\nu}(\mathbf{R})\right]\exp(\mathrm{i}\mathbf{kR})\,\frac{\mathrm{d}^3\mathbf{k}}{(2\pi)^3}\right\}. \tag{17}$$

Here M is the proton mass, $\mathbf{e}(\mathbf{q}, \lambda)$ is the phonon polarization vector, and $\lambda_{\alpha\beta}(\mathbf{R})$ is the pair correlation function of displacements. In the quasiharmonic approximation, $\lambda_{\alpha\beta}(\mathbf{R})$ may be written as

$$\lambda_{\alpha\beta}(\mathbf{R}) = \frac{1}{M}\sum_{\mathbf{q},\lambda}\left[1-\cos(\mathbf{qR})\right]e_\alpha(\mathbf{q},\lambda)e_\beta(\mathbf{q},\lambda)\omega^{-1}(\mathbf{q},\lambda)\,. \tag{18}$$

Equations (17), (18) are solved self-consistently. This means that first the phonon frequencies and polarization vectors are found. Then, the correlation function of displacements $\lambda_{\alpha\beta}(\mathbf{R})$ is determined. After that the renormalized force constants are calculated, and the whole cycle is iterated to self-consistency. In Ref. [50] the Coulomb potential screened by free electrons, which have the dielectric function $\varepsilon(\mathbf{k})$, was used as an initial proton-proton interaction. Then, the effect of phonons on the electron contribution to energy was taken into account [50]. The resulting potential $U(R)$ was presented in the form

$$U(\mathbf{R}) = \int \frac{4\pi e^2}{k^2\varepsilon(\mathbf{k})}\exp\left[-\frac{1}{2}\,k_\alpha k_\beta\lambda_{\alpha\beta}(\mathbf{R})\right]\exp(\mathrm{i}\mathbf{kR})\,\frac{\mathrm{d}^3\mathbf{k}}{(2\pi)^3}\,. \tag{19}$$

In the harmonic approximation, i.e., assuming that $\lambda_{\alpha\beta}(\mathbf{R}) = 0$, Eqn (16) transforms to the standard expression for the metal energy in terms of the second-order perturbation theory in electron-ion (proton) potential [8].

Subsequently, the same method for calculating the quasiharmonic phonons was applied [51] to study the molecular phase. In this case, however, the initial interprotonic potential $V_0(\mathbf{R}_n, \mathbf{R}_{n'})$ was calculated within the DFT. Then the phonon frequencies determined in such a way were used to calculate the zero-point energy that was, in turn, included into the total energy of crystal. In a number of investigations (for example, Refs [31, 52]) the zero-point energy was calculated in the harmonic approximation. The conclusions made in Refs [31, 52] imply that the ZPM must be taken into account in the determining the crystal structure energies and that its inclusion may change the sequence of structures arranged by total energy, which is essential in finding the ground state of the system.

An attempt to take into account the dynamics of proton vibrations in the crystalline potential was made in the calculations [40, 46] performed by the AIMD method. This approach was advanced for the first time by Car and Parrinello [53]; its essence is as follows. Classical molecular-dynamics simulation of a system with the Hamiltonian

$$H = \sum_n \frac{\mathbf{p}_n^2}{2M} + \frac{e^2}{2}\sum_{n,n'}\frac{1}{|\mathbf{R}_n - \mathbf{R}_{n'}|} + E_{\mathrm{el}}\{\mathbf{R}_n\}\,, \tag{20}$$

is performed. Here $\mathbf{p}_n$ is the particle momentum and M is its mass (proton mass in our case). The electron contribution to the Hamiltonian $E_{\mathrm{el}}\{\mathbf{R}_n\}$ is calculated within the DFT described above. Thus, the electron energy is determined self-consistently for any position of protons. Then, the forces acting on the protons are calculated by the classical Newton equations.

Among the drawbacks to the outlined approach are, of course, all those mentioned above in connection with the DFT. There are also inaccuracies specific to the AIMD method. First, the number of particles involved in molecular-dynamics simulation is rather small. As a rule, it does not exceed 128 atoms. The second essential shortcoming is related to the way of calculating the electronic energy. Usually it is calculated by integration over the momentum space. Integration over the real space is, in turn, most commonly replaced by taking an integral over a small number of points in the momentum space. In many studies this number was simply equal to 1, i.e. $\mathbf{k} = 0$. In Ref. [40] it was demonstrated that this approach might introduce large errors, even into the evaluation of the crystal structure energy.

The quantum Monte Carlo method is best suited to take into consideration all the peculiarities of crystalline hydrogen behavior under high pressure. Only a few calculations of solid hydrogen performed by this method are currently available [32 – 34, 47, 48]. In Ref. [47] the properties of high-density hydrogen are calculated by a generalized Car – Parrinello AIMD method developed in [54, 55] to take into account the quantum character of proton motion. Broadly speaking, the essence of this generalization boils down to the calculation of the partition function for the proton quantum system described by Hamiltonian (20). This partition function is written as a path integral with subsequent replacement of the latter by an ordinary integral over a large number of variables. Each proton is represented by a ring polymer of classical particles with a finite number of 'beads' that is equal to the number of discretizations in imaginary time. The mathematical Monte Carlo method is used to calculate the resulting integrals. The results [47] make it clear that taking into account the quantum behavior of protons is of great importance. Thus, at low temperatures of ~ 50 K the pair correlation function of quantum protons $g(r)$ is demonstrated [47] to have the shape closely similar to the $g(r)$ of classical protons at $T = 520$ K. This, in particular, indicates a large amplitude of the protonic ZPM. In Refs [32, 33] molecular hydrogen was calculated in the pressure range 100 to ~ 250 GPa by means of a quantum Monte Carlo method with both protons and electrons treated on equal footing, that is their quantum motion was taken into complete account. The simulations were performed for 48 molecules. As was pointed out above, the results of these EOS calculations turned out to be different by $\sim 8\%$ from experimental data, regarding the determination of specific volume.

We now proceed to discuss the theoretical calculations of the crystal structure and properties of molecular hydrogen at pressures corresponding to phases II and III. Figure 3 displays some candidate structures for these phases. In these structures, the molecular centres occupy the sites of the hcp lattice. The simplest of them considered first in Ref. [2] and then investigated thoroughly in Ref. [31] is shown in Fig. 3a. In this structure, sometimes referred to as mhcp-c, the axes of all molecules are aligned parallel to c. However, a detailed consideration [43 – 45] of the stability of various structures, and of their energies, performed on the basis of band structure calculations demonstrated that the low-coordinated, so-called 'canted', structures are more stable and have lower energy. Figures 3b, c display two such structures characterized by orthorhombic symmetry. One of these structures corresponding to the space group $Pca2_1$ (Fig. 3b) possesses the lowest energy among the systems of classical quadrupoles, as was earlier demonstrated by Kitaigorodskii and Mirskaya [52]. In this structure, the molecular axes lie along four directions according to the combinations of $\cos\theta \cong \pm 1/\sqrt{3}$ and $\cos\varphi \cong \pm 1/\sqrt{2}$, with the polar angle θ measured from the c axis, and the azimuthal angle φ measured from the direction to the nearest molecule. The structure shown in

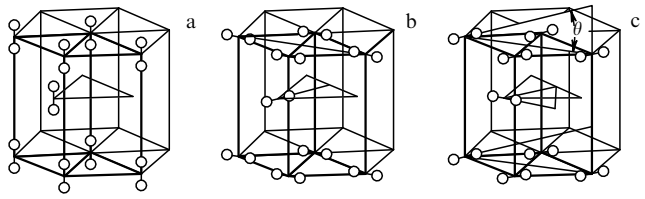

Figure 3. Predicted hcp-type crystal structures for molecular hydrogen: *c*-axis oriented molecules [2, 31] (a); the axes of molecules lie on the *ab* plane [43] (b); molecules are tilted off the *ab* plane [43, 44] (c).

Fig. 3c has the space group $Cmc2_1$. In its two sublattices moved relative to each other by $c/2$, the molecular axes are tilted from the c axis by the angles θ and $-\theta$, correspondingly, with $\theta \approx 30°$.

The $Pca2_1$ structure (Fig. 3b) is the strongest candidate for a crystal structure of phase II. This conclusion stems from a detailed consideration [40] of energies and lattice dynamics performed by the AIMD method for several crystal structures in the corresponding pressure range. First, it was shown in Ref. [40] that within the classical treatment of proton dynamics, this structure has the lowest energy among all other structures considered. A system ordered initially in an arbitrary lattice relaxes to the $Pca2_1$ structure in the course of molecular-dynamics simulation. Second, this structure possesses optically active modes, which are found experimentally to appear at the phase I - phase II boundary. This is no surprise, since the molecules in this structure may possess quadrupole moments by virtue of $Pca2_1$ symmetry. Occurrence of the quadrupole moments Q leads [39] inevitably to electric fields $E \sim \beta Q/a^4$ occurring in the system, here β is some number depending on the structure and orientation, and a is the lattice parameter. The electric fields give rise, in turn, to the effective charges $q \sim \alpha E/d$ occurring in the molecules, here α is the molecular polarizability and d is the molecular bond length. An essential problem, which, however, has not been comprehensively studied, is the mechanism for occurrence of the quadrupole moments in hydrogen molecules. It remains unclear whether they are trivially caused by the crystalline field or the quadrupole moments due to the ortho-states of hydrogen molecules are also observed in real experiments as, actually, assumed in Ref. [39].

In phase II, the effective charge of optically active vibrons is extremely small, $q \approx 0.004e$, where e is the electron charge. In phase III it increases almost by two orders of magnitude. In Ref. [39] it was noted that in phase III the integrated intensity of IR absorption is proportional to the squared shift $(\Delta\nu)^2$ of the vibron frequency, where $\Delta\nu$ is measured with respect to the frequency value at the transition point. This may be an indication that the both quantities, q and $\Delta\nu$, depend on a single order parameter characteristic of phase III and are proportional to it. It is suggested in Ref. [39] to consider the quadrupole moment of molecule as such a parameter. This interpretation of the phase III properties was challenged [41, 57] and models were proposed [41, 57] for the crystal structure of phase III, whereby the hydrogen molecules get dipole moments, i.e., the electron charge is transferred within a molecule from one proton to another, and the molecule acquires some fraction of an ionic bond. A previous assumption [58] is noteworthy that at high compressions molecular hydrogen may become a fully ionic compound (of NaCl type). Previously, a hypothetical ionic phase of atomic hydrogen was examined and found to be not favored energetically [59].

Edwards and Ashcroft [41] considered the structures $Cmc2_1$ (see Fig. 3c) and $C2/m$ as candidates for phase III. The $C2/m$ structure possesses monoclinic symmetry and is different from $Cmc2_1$ in that the molecular axes in both sublattices are parallel, i.e. all are tilted from the c axis by the angle $\theta \approx 30°$. It was shown on the basis of band structure calculations that at a small sliding of either sublattice in the plane perpendicular to c, the charge distribution along the molecular bond becomes asymmetric in both structures. It was also shown that the structure $Cmc2_1$ distorted by such a displacement possesses a lower energy than $C2/m$. In this work, the effective dipole charge and the shift of vibron modes $\Delta\nu$ were not calculated in detail. Nevertheless, simple estimates [41] show that this model is, at least, not contrary to the interrelation between q and $\Delta\nu$ observed experimentally. It should be noted that in the $Cmc2_1$ structure distorted by sublattice displacement, the number of optically active modes exceeds that observed experimentally (2 instead of 1). The authors of Ref. [41] also point out that in the $C2/m$ structure which, according to their calculation, has a higher energy the number of IR- and Raman-active phonons is in agreement with the experimental data. In this connection, study [47] should be mentioned, where the crystal structure of hydrogen was calculated by the quantum Monte Carlo method at various pressures. A structure qualitatively similar to $C2/m$ was shown in [47] to possess the lowest energy. However, its characteristics, such as the tilting angles of molecules, the molecular bond length and the lattice parameters are slightly different from those obtained by Edwards and Ashcroft [41]. A detailed investigation of optical-mode frequencies in high-density hydrogen was performed by the Japanese team [45] with the use of DFT and a standard method of band structure calculation. They calculated the optical-mode frequencies and their dependence on pressure for three structures — $Pca2_1$, $Cmc2_1$ and $Cmca$ — and demonstrated that the vibration frequencies obtained for the $Pca2_1$ structure are in close agreement with the experimental data. This confirms the results reported previously in Ref. [41]. According to calculations [45], the $Cmc2_1$ is the strongest candidate for phase III.

The problem of effective dipole charges in phase III was studied most comprehensively by Souza and Martin [57]. They considered the $C2/m$ and $Cmc2_1$ structures as well. Based on band structure calculation, they found not only the charge distribution in the system but also the electric polarization related to the IR-active vibron modes. For this purpose, the Berry's phase [60] formed of electron wavefunction phases was used to describe the polarization of the periodic insulating system. It follows from calculation [57] that at pressures corresponding to phase III the effective charges in $C2/m$ structure are almost thirty times larger than those observed experimentally. Moreover, in this structure the band gap is closed at pressures of ~ 160 GPa and the system transforms to a metallic state. In the $Cmc2_1$ structure band-gap closure does not take place up to the highest pressures considered in this work (~ 180 GPa) which is in agreement with the results [41, 42]. The calculated effective charges, however, are several times larger than the experimental ones.

The following conclusions can be made from the above discussion on the structure and properties of high-pressure

molecular hydrogen. The main point is the inadequacy of available *ab initio* methods to explain hydrogen's properties. The fact that uncertainties and errors of different kinds arise in studies of crystal properties by these methods [61] has been well known for a long time. These errors are rather small for many crystalline systems and do not substantially affect the results of calculations of their properties. In this regard, high-pressure hydrogen turned out to be a very special system: it may form many crystal structures of nearly the same energy which are, however, highly distinct in other characteristics, as the $C2/m$ and $Cmc2_1$ structures exemplify. For instance, at $p \approx 160$ GPa hydrogen becomes a metal in the $C2/m$ structure, while it remains an insulator in the $Cmc2_1$ structure. Moreover, many quantities including the effective charges depend strongly on the lattice constant and the molecular bond length, so an error of several percent in determining these parameters may result in a much more considerable change in the charge magnitude. It is clear that a further increase in the accuracy of *ab initio* calculations is needed to evaluate reliably the properties of high-pressure hydrogen. It is not only in the case of hydrogen that this task may become urgent. There is recent experimental and theoretical evidence [62] that pressurized crystalline lithium also exhibits various anomalies including the occurrence of the same complex crystal structures and even a possible transition of lithium into an insulating state with increasing pressure.

3. Insulator – metal transition

In the physics of hydrogen, a long-standing problem, however, still unsolved, is the insulator – metal (IM) transition at high pressure. This problem became a subject of vigorous study, both theoretical and experimental, in the 70s. At that time, several experimental observations of IM transition were reported [13, 14, 23, 63, 64]. In two of those experiments [63, 64], two different static-pressure devices were used. In the experiment performed by a group from the High Pressure Physics Institute headed by Vereshchagin [63] a hydrogen sample was placed on a flat anvil of polycrystalline diamond and pressed by a thin indenter also made of polycrystalline diamond. In the experiment carried out by a Japanese team [64] a hydrogen sample was placed inside a nine-sector sphere made of tungsten carbide, and high pressure was generated by bringing these sectors synchronously together. In Ref. [63] the indenter-to-anvil voltage was measured, and the IM transition was detected through a drastic decrease in voltage at some compression. The corresponding value of pressure was estimated with a high degree of uncertainty. Actually, a question arose as to whether or not the observed drastic decrease in voltage was caused by the puncture of a hydrogen sample with diamond indenter. The work by Japanese investigators [64] provoked much criticism as well. Thus, it still remains unclear whether the IM transition of hydrogen was really observed in these experiments. Utter denial of this fact does not nowadays seem to be so convincing as it was in the 70s. The point is that the same group from HPPI observed an IM transition in crystalline sulphur [65]. Moreover, a subsequent transition of metallic sulphur to a superconducting state was observed. Those results received initially with profound skepticism have recently been confirmed by investigations made with diamond-anvil cells [66, 67].

Observations of IM transitions were also reported in early shock-compression experiments [13, 14]. These investigations were performed in nuclear centres of the USSR (Arzamas-16) [13] and USA (Lawrence Livermore National Laboratory, LLNL) [14]. In these experiments, isentropic shock compression was used to lower hydrogen temperatures as compared to those arising at ordinary shock compression. For this purpose, a metallic shell enclosing a hydrogen sample was compressed by means of high magnetic fields produced by explosion. The idea of explosive compression used to create high magnetic fields was advanced in the USSR by Andreĭ Sakharov [68]. The Arzamas-16 investigators determined the density of hydrogen by measuring the diameter of a cylindrical enclosure containing a hydrogen sample with a powerful transmission γ-spectrometer. The American team measured, besides density, the electrical resistance of hydrogen. In fact, no thermodynamic variable other than density was measured in both experiments. Only the speeds of shock waves generated in the experiments can be reconstructed. All other quantities are to be calculated using various phenomenological equations of state and the shock wave theory. As mentioned in the preceding section, the Arzamas-16 team managed to reconstruct the EOS of molecular hydrogen to pressures of ~ 400 GPa surprisingly well. In Ref. [13], several possible pressures corresponding to different equations of state for the molecular phase are reported for a transition registered through an abrupt change in density. When using one set of parameters [23] that leads to the best agreement with the EOS to 120 GPa known today, the transition observed by this group takes place around 400 GPa. The American investigators reported in their publication an IM transition registered around 200 GPa. According to their measurements, the electrical conductivity of hydrogen was of the order of $1\ \Omega^{-1}\ \mathrm{cm}^{-1}$ which is considerably lower than the threshold of metallic conductivity. In Ref. [14], the EOS was not established with sufficient reliability.

We shall subsequently return to an extended discussion of the work by the Arzamas-16 investigators, and here we mention only that new observations of the IM transition in hydrogen at shock compression have been recently reported by a Livermore team [69].

As is evident from the above discussion, the experimental observation of the IM transition in high-density hydrogen is an extremely complicated problem that still remains unsolved. A similar statement is true for theoretical calculation of this transition as we shall see later. In early publications [1 – 4], the IM transition was customarily associated with the transformation of hydrogen from a molecular state to an atomic one. As was noted subsequently [70, 71], the metallization of high-density hydrogen should most probably occur in its molecular phase, owing to the overlap of electron bands and the closure of an indirect band gap. Such a phenomenon was observed, for example, in molecular iodine [72]. Subsequent extended calculations [42, 44, 52, 73] confirmed the assumption that the IM transition may occur in the molecular phase of hydrogen.

The possible pressure of this transition is easily estimable by means of various techniques. The IM transition in the molecular phase takes place if the widths of both filled $1\sigma_g$ and empty $1\sigma_u$ bands originating from the corresponding molecular orbitals exceed the splitting of these bands. An estimate [73] made using the tight-binding method with variational Slater 1s orbitals indicates that this overlap should occur at densities corresponding to $r_s = 1.45$, which

corresponds to pressures of the order of 150 GPa. The parameter r_s is the radius of a sphere falling at one electron:

$$\Omega_0 = \frac{4\pi}{3} r_s^3 r_B^3 , \tag{21}$$

where Ω_0 is the volume per electron and r_B is the Bohr radius.

Another way of estimating the transition pressure is based on a longstanding idea [74] of a so-called 'dielectric catastrophe'. Let us write the dielectric function of molecular crystal in the Lorenz – Lorentz form:

$$\varepsilon = 1 + \frac{4\pi n\alpha}{1 - 4\pi n\alpha/3} , \tag{22}$$

where n is the density of molecules and α is their polarizability. The IM transition may be expected to occur, as ε goes to infinity. This takes place under the following condition:

$$\frac{4\pi n\alpha}{3} = 1 . \tag{23}$$

According to a simple estimate [41] made using the α value for a free molecule, equality (23) is again true at $p \sim 150$ GPa. With this estimate, it is no wonder that the transition between phases II and III that takes place just at $p \approx 150$ GPa was initially thought of as the onset of hydrogen metallization [37].

On the one hand, the extended calculations [42, 44, 52, 73] mentioned above demonstrated, that the cited simple estimate of the IM transition pressure in the molecular phase was reasonable. Indeed, according to these calculations the pressure of the IM transition falls in the range 130 to 180 GPa for many molecular crystal structures. On the other hand, these very calculations revealed a number of difficulties in the solution of this problem. First of all, it was found that the IM transition pressure might depend strongly on the crystal structure of molecular hydrogen. To be more exact, it depends on the orientation of the molecular axes, since most of the crystal structures favored energetically have an hcp-like arrangement of molecular centres. Moreover, lower pressures of IM transition are inherent in the very structures, which are less preferred energetically in the insulating state. An example is the mhcp-c structure with all molecular axes aligned parallel to c. According to the band structure calculation [43] made within the DFT, this structure has the highest energy as compared to all other hcp-based structures and the smallest energy gap at the same density. Its metallization pressure turns out to be the lowest as well.

Figure 4 illustrates in a more informative way the positions of hydrogen molecules in the three crystal structures presented schematically in Fig. 3, while the relative energies of these structures and the corresponding energy gaps are presented in Fig. 5 (both Figs 4 and 5 are after Ref. [43]). Figure 5 demonstrates clearly that the mhcp-c structure has, indeed, the smallest gap, but it is not favored energetically within a large compression range. The calculation [43] was performed in the clamped-nuclei approximation, i.e. without including ion vibrations. More recently, it was shown [52] that the situation could be changed considerably by taking into account the phonon contribution to the total energy of crystal. Figure 6 (after Ref. [52]) exhibits the relative energies of the structures with different θ angles by which the molecules are tilted to the c axis. Notice, that the $\theta = 0$ case corresponds to the structure in Fig. 4a, and the $\theta = 60°$ structure is that of Fig. 4c. It is seen in Figure 6 that inclusion

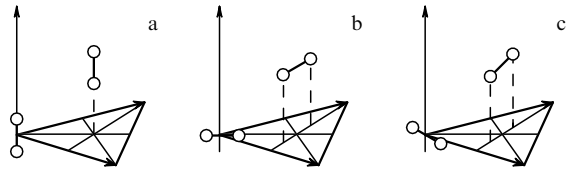

Figure 4. Three molecular orientations a, b and c corresponding to the three structure types in Fig. 3a, b, c. The arrows represent the basis vectors of the hcp lattice.

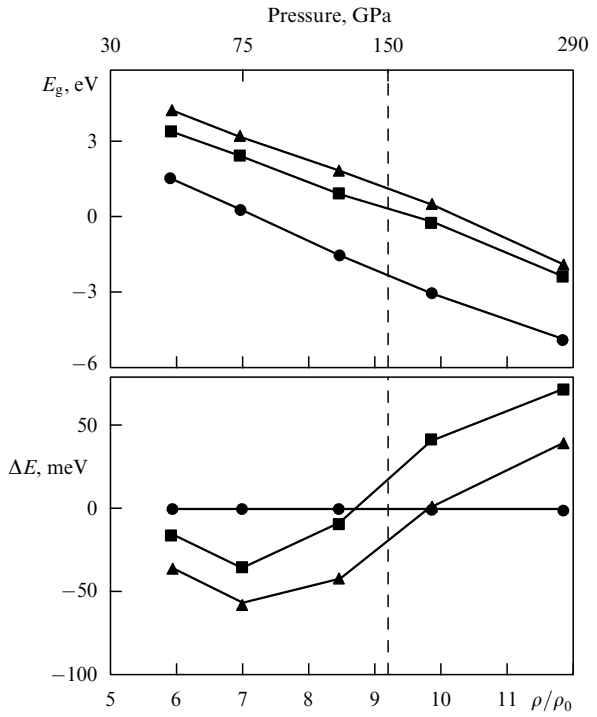

Figure 5. Indirect band gap (top panel) and comparison between total energies per hcp unit cell for three molecular orientations (bottom panel). The circles, squares, and triangles correspond to the molecular orientations in Fig. 4a, b, c, respectively. The pressure values (top scale) are obtained from the experimental equation of state [18, 19, 21]. The vertical dashed line indicates the experimental vibron discontinuity pressure.

of the zero-point contribution alters the relative energies of phases, and the $Pca2_1$-to-mhcp-c crystallographic transition should occur at $p \approx 78$ GPa. According to the calculation under discussion, this transition would probably be accompanied by the IM transition because the mhcp-c phase is metallic at such pressures. It is known to a high degree of certainty that the IM transition does not actually occur either at such pressures or at considerably higher pressures up to 300 GPa.

It follows from the above discussion that a whole set of intricate problems arise, when evaluating the metallization pressure of molecular hydrogen. First, the accurate evaluation of the energy gap and of the pressure (or, at least, density) at which the gap is closed, i.e. the IM transition occurs, is necessary. Second, an accurate calculation is required of relative energies for different crystalline phases, in both insulating and metallic states. Third, one should take into account the effect of phonons on the crystalline phase energy,

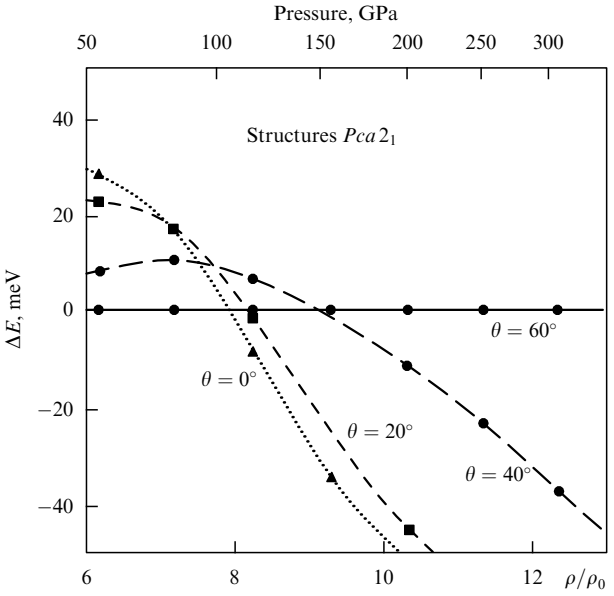

Figure 6. Total energies per molecule of $Pca2_1$-type phases (including vibron zero-point energy) as related to the energy of the $\theta = 60°$ phase.

as well as on its electronic structure, in particular, on the energy gap. It will be seen later that the solution of all these problems is presently hindered by the lack of a detailed underlying theory.

Let us start our consideration with the gap problem. The DFT outlined in the preceding section of this review provides a standard approach for calculating the energy band structure of crystals, that has been used in most of the studies on molecular hydrogen [41, 42, 51, 73]. This approach reduces to solving the Kohn–Sham equations (12)–(14). The band structure described by the dispersion law $\varepsilon_{\mathbf{k}\lambda}$ ($\mathbf{k}$ is the wave vector in the first Brillouin zone and λ is the number of a branch of the electronic spectrum) is a result of solving these equations. Figure 7 displays the band structure of molecular hydrogen calculated in Ref. [42]. The calculation is performed at a hydrogen density corresponding to $r_s = 1.6$. The above-mentioned strong crystal-structure dependence of the band structure and, in particular, of the energy gap is clearly visible from Fig. 7. Thus, at $r_s = 1.6$, the indirect gaps are closed in the mhcp-*c* phase, and the system becomes a zero-gap semiconductor, while the $Cmc2_1$ phase remains an insulator with rather a large gap, $E_g \approx 1.5$ eV. It should be noted that in the *Cmca* phase, the gaps are closed at lower density, and this phase is already metallic at $r_s = 1.6$. The *Cmca* structure was not considered in Ref. [43] where the mhcp-*c* phase was reported to possess the lowest metallization pressure.

It was established in Refs [75, 76] that in the framework of DFT, the energy gap is, in principle, underestimated for insulating systems. This is related to the so-called discontinuity of the exchange-correlation potential. We will not discuss this problem in detail here, referring the interested reader to review [77]. Two points, however, should be emphasized. First, the gap is underestimated not only in the local density approximation, but in the case of the exact exchange-correlation potential as well [77]. Second, as demonstrated in Ref. [7], the DFT underestimates not only the gap value at any given density, but also the density value at which this gap is closed. Thus, the DFT underestimates the value of pressure at which the IM transition occurs.

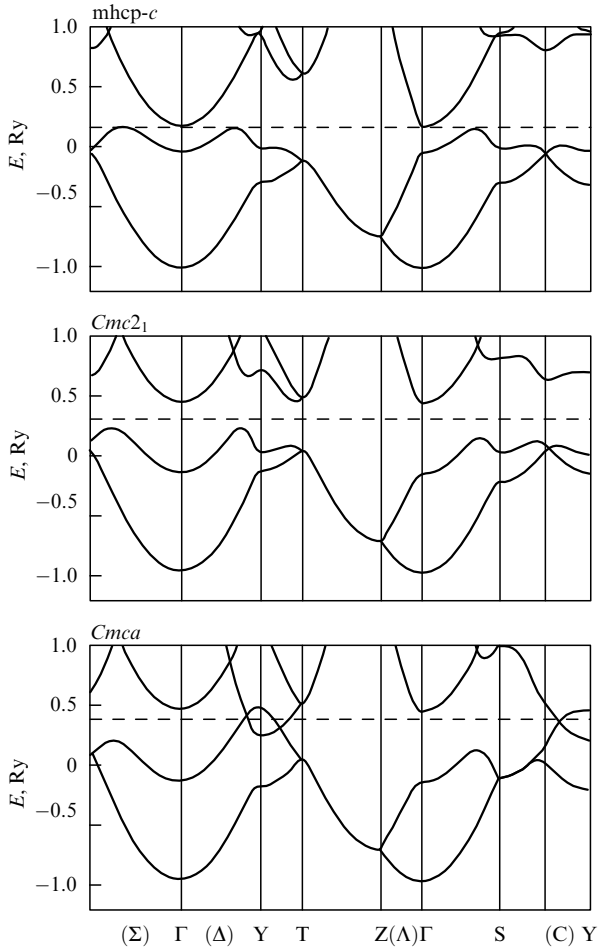

Figure 7. Band structure for the $Cmc2_1$, *Cmca*, and mhcp-*c* phases at $r_s = 1.6$. The molecular bond length is set at 1.40 r_B for all structures and the molecular orientation is set at $\theta = 60°$ for the $Cmc2_1$ and *Cmca* structures.

The band gap of insulators is to be found not by solving the Kohn–Sham equations (12)–(14), but by the use of a one-particle Green's function. An appropriate equation has the following form:

$$\left[-\frac{\nabla^2}{2m} + \sum_n V_n(\mathbf{r} - \mathbf{R}_n) + e^2 \int \frac{\rho(\mathbf{r}')}{|\mathbf{r} - \mathbf{r}'|}\, d\mathbf{r}'\right] \psi_{\mathbf{k}\lambda}(\mathbf{r}) + \int \Sigma(\mathbf{r}, \mathbf{r}', \varepsilon_{\mathbf{k}\lambda}) \psi_{k\lambda}(\mathbf{r}')\, d\mathbf{r}' = \varepsilon_{\mathbf{k}\lambda} \psi_{\mathbf{k}\lambda}(\mathbf{r})\,. \quad (24)$$

The only but essential difference between this equation and the Kohn–Sham one (12) is in the fourth term in the left-hand side of Eqn (24). Instead of a local operator of exchange-correlation potential $V_{xc}(\mathbf{r})$, a non-local energy-dependent operator of self-energy $\Sigma(\mathbf{r}, \mathbf{r}', \omega)$ appears in the equation for one-particle excitations.

It is easy to understand that the electron bands obtained from these two equations may be substantially different, even in the simplest case of the homogeneous electron gas. In this case $V_{xc}(\mathbf{r})$ is merely a constant, and the spectrum obtained from the corresponding Kohn–Sham equation coincides with the spectrum of non-interacting electrons. The situation is completely different in the case of one-particle excitations determined by Eqn (24). First of all, the electron mass is

renormalized in the vicinity of the Fermi surface. Moreover, the excitations have a finite lifetime due to the imaginary part of $\Sigma(\mathbf{k}, \omega)$.

Going to the consideration of crystalline systems, we note, first of all, that the solution of the Kohn–Sham equations with the local operator $V_{xc}(\mathbf{r})$ alone is a nontrivial procedure for three-dimensional crystals. It is clear that the solution of Eqn (24) presents an even more considerable challenge. But this is apparently not the crux of the difficulty in the calculation under discussion. Evaluation of the self-energy $\Sigma(\mathbf{r}, \mathbf{r}', \omega)$ on its own presents the central problem. Usually, when doing such a calculation, one restricts oneself to the simplest approximation referred to as the GW approximation and written in the form [79]

$$\Sigma(\mathbf{r}, \mathbf{r}', \omega) = +\frac{\mathrm{i}}{2\pi}\int W(\mathbf{r}, \mathbf{r}', \omega) G(\mathbf{r}, \mathbf{r}', \omega - \omega')\, \mathrm{d}\omega' \qquad (25)$$

where $G(\mathbf{r}, \mathbf{r}', \omega)$ is a one-particle Green's function satisfying the following equation:

$$\left[\omega - \frac{\nabla^2}{2m} + \sum_n V_n(\mathbf{r} - \mathbf{R}_n) + e^2\int \frac{\rho(\mathbf{r}')}{|\mathbf{r} - \mathbf{r}'|}\, \mathrm{d}\mathbf{r}'\right] G(\mathbf{r}, \mathbf{r}', \omega) + \int \Sigma(\mathbf{r}, \mathbf{r}'', \omega) G(\mathbf{r}, \mathbf{r}'', \omega)\, \mathrm{d}\mathbf{r}'' = \delta(\mathbf{r} - \mathbf{r}')\,. \qquad (26)$$

and $W(\mathbf{r}, \mathbf{r}', \omega)$ characterizes the electron-electron interaction and has the form of a screened Coulomb potential:

$$W(\mathbf{r}, \mathbf{r}', \omega) = e^2\int \frac{1}{|\mathbf{r} - \mathbf{r}''|}\, \varepsilon^{-1}(\mathbf{r}'', \mathbf{r}', \omega)\, \mathrm{d}\mathbf{r}''\,. \qquad (27)$$

Here $\varepsilon^{-1}(\mathbf{r}, \mathbf{r}', \omega)$ is an inverse electron dielectric function (DF) of crystal. It is commonly determined in the framework of the simplest random phase approximation:

$$\varepsilon(\mathbf{r}, \mathbf{r}', \omega) = \delta(\mathbf{r} - \mathbf{r}') + e^2\int \mathrm{d}\mathbf{r}' \int \mathrm{d}\mathbf{r}''\, \mathrm{d}\omega' \frac{1}{|\mathbf{r} - \mathbf{r}''|} \times G(\mathbf{r}', \mathbf{r}'', \omega - \omega') G(\mathbf{r}'', \mathbf{r}', \omega')\,. \qquad (28)$$

Calculation of the DF from equation (28) with a subsequent change to the momentum representation, i.e. derivation of the $\varepsilon(\mathbf{q} + \mathbf{K}, \mathbf{q} + \mathbf{K}', \omega)$, matrix ($\mathbf{K}$ and $\mathbf{K}'$ are vectors of reciprocal lattice), allows one to find an inverse matrix $\varepsilon^{-1}(\mathbf{q} + \mathbf{K}, \mathbf{q} + \mathbf{K}', \omega)$.

The above approach to the calculation of the spectrum of electron excitations was successfully applied to a number of semiconductors and insulators [80]. A few simplifications to this approach were also suggested which allowed such calculations to be performed more efficiently. Thus, a Green's function derived in the framework of DFT rather than the self-consistent Green's function from equation (26) was proposed [81] for use when calculating the self-energy (25):

$$G(\mathbf{r}, \mathbf{r}', \omega) = \sum_{\mathbf{k}, \lambda} \frac{\psi^*_{\mathbf{k}\lambda}(\mathbf{r})\psi_{\mathbf{k}\lambda}(\mathbf{r}')}{\omega - \varepsilon_{\mathbf{k}\lambda}}\,. \qquad (29)$$

Various simplified techniques were also proposed for calculating the inverse DF (see, for example, Ref. [82]). The simplest way to find the excitation spectrum of an insulator was suggested in Ref. [78]. It was demonstrated on the basis of analytical consideration of the expression (25) for self-energy that the main distinction of $W(\mathbf{r}, \mathbf{r}', \omega)$ from the local exchange-correlation potential is the exchange interaction nonlocality describable within the Hartree–Fock approximation. It was suggested that a correction to the excitation energy be sought

$$\Delta E_{\mathbf{k}\lambda} = E_{\mathbf{k}\lambda} - \varepsilon_{\mathbf{k}\lambda}\,, \qquad (30)$$

where the energy $E_{\mathbf{k}\lambda}$ is a solution to equation (24) and $\varepsilon_{\mathbf{k}\lambda}$ is the energy in DFT, in the following form:

$$\Delta E_{\mathbf{k}\lambda} = \frac{E^{\mathrm{HF}}_{\mathbf{k}\lambda} - \varepsilon_{\mathbf{k}\lambda}}{\varepsilon_0}\,. \qquad (31)$$

Here $E^{\mathrm{HF}}_{\mathbf{k}\lambda}$ is the Hartree–Fock excitation energy (the gap is overestimated in this approximation), and ε_0 is the static electron DF. Both the energy gap and the near-gap excitation spectra obtained in these calculations [78] turned out to be in excellent agreement with the experimental data. The GW approximation was also applied to evaluate the energy gap and the metallization pressure in molecular hydrogen [83]. The metallization pressure was demonstrated to be nearly twice as high as that obtained within the DFT approach.

Turning back to the second of the above problems arising in the calculation of the metallization pressure for molecular hydrogen, namely, to the necessity of precisely calculating the crystal structure energies, we will only add something to what has been said in the preceding section concerning the inaccuracy of the methods used. This 'something' is concerned with the probable inconsistency when using the two approaches. As pointed out already, the metallization pressure should be calculated from the equation for the one-particle Green's function rather than within the DFT approach. In this case, it would be natural to use the Green's function method in the calculation of the relative energies as well. To date, however, such attempts have not been made for crystalline systems. The GW method has only been recently applied to calculate the energy of the homogeneous electron gas [84]. So far, a generalization of this method to crystalline systems is lacking.

To conclude the discussion on the calculation of the metallization pressure in the molecular phase, we briefly discuss the role possibly played by phonons and by electron-phonon interaction in this problem. So far, when calculating the metallization pressure, the phonon effect has been taken into account only through the inclusion of the zero-point contribution to the total energy of crystal [52]. It is well known, however, that the consideration of the electron-phonon interaction within the many-body theory [85] can change the gap width, as well as its dependence on density and temperature [86]. As yet, no adequate technique has been developed to take into account those effects in the framework of DFT, while, considering the strong dependence of the energy gap on the crystal structure in molecular hydrogen, it is beyond question that the gap width can be substantially changed just through the electron-phonon interaction.

Evidence in favor of this fact is, perhaps, the observation of the IM transition in liquid hydrogen at pressures of ~ 140 GPa and temperatures of ~ 2600 K reported in Ref. [69]. The measurements were carried out using strong shock waves generated by a hypervelocity impactor made of Al or Cu. A layer of liquid hydrogen placed between Al_2O_3 anvils was held by two Al plates cooled to 20 K. On impact of the impactor onto the Al plate, a strong shock wave is created which travels

through the hydrogen layer to compress it. To decrease the temperature occurring in the hydrogen sample, compression by shock waves reverberating between the Al_2O_3 anvils was used. The experimental set-up also incorporated electrodes to measure the electrical resistivity of the compressed hydrogen sample. The set-up components are described in detail in Ref. [69]. The parameters of the Hugoniot shock adiabat measured in the case of reverberating shock waves are not too different from those measured before by the group from Arzamas-16 [13, 23]. However, no abrupt first-order phase transition was observed in the experiment [69] under discussion. In this experiment, the electric conductivity of hydrogen was found to increase monotonically through four orders of magnitude in the pressure range 93 to 140 GPa and to be constant and approximately equal to $2000\ \Omega^{-1}\ \mathrm{cm}^{-1}$ in the range 140 to 180 GPa. This conductivity is of the same order as that of dense Cs and Rb vapors at the IM transition in the temperature range ~ 2000 K [87].

The experimental data on electric conductivity in the pressure range 93 to 140 GPa were approximated by a standard expression for conductivity in semiconductors:

$$\sigma = \sigma_0 \exp\left(-\frac{E_g}{2k_B T}\right). \tag{32}$$

Here the value of σ_0 and the energy gap E_g are considered to be dependent on the density ρ and are fitted to the experimental data. Moreover, in the specified pressure range, the conductivity is reasonably well approximated with a linear ρ-dependence of E_g:

$$E_g(\rho)\ [\mathrm{eV}] = 1.22 - 62.6(\rho - 0.30)\,. \tag{33}$$

Here ρ is expressed in mole cm^{-3}, and σ_0 is assumed to be constant and equal to $90\ \Omega^{-1}\ \mathrm{cm}^{-1}$. The rate of gap reduction with increasing density is equal to 62.6 eV $\mathrm{mole}^{-1}\ \mathrm{cm}^3$ which is rather close to that calculated theoretically [83] in the case of solid hydrogen (40 eV $\mathrm{mole}^{-1}\ \mathrm{cm}^3$). The gap expressed in temperature units becomes equal to approximately 2600 K at the density of 0.32 mole cm^{-3} corresponding to a pressure of 120 GPa. Thus, in the opinion of the authors of Ref. [69], a complete IM transition ($E_g = 0$) occurs in liquid hydrogen at $p = 140$ GPa and $T = 2600$ K. At higher pressures, the electric conductivity becomes practically pressure-independent.

So, in accordance with the results [69], the hydrogen metallization pressure decreases considerably in the fluid phase. This is of course related largely to the strong crystal-structure dependence of this pressure. In the above-cited theoretical papers it was demonstrated that the mhcp-*c* structure possesses the lowest pressure of metallization, p_c. The canted structures have higher p_c values. However, in Ref. [83] it was shown using a 'virtual-crystal approximation' that the metallization pressure decreases to approach p_c for the mhcp-*c* structure if the disordering of molecular axes is taken into account.

Notice that there is serious disagreement on the theoretical interpretation of the very process of metallization found experimentally to occur at $p_c = 140$ GPa and $T_c = 3000$ K. Based on molecular-dynamics simulation [88], the experimenters themselves consider hydrogen near the metallization point to be essentially 'molecular': the fraction of dissociated molecules is 10% or even less. However, another theoretical study [89] also performed with the use of molecular dynamics method states that, in fact, the metallization observed in Ref. [69] occurs simultaneously with the progressive dissociation of molecules to atoms. One probable reason for the disagreement between these two works has to do with different calculational techniques. In Ref. [89], the *ab initio* Car–Parrinello method [53] was used, while in Ref. [88] a semi-phenomenological approach based on the tight-binding method was applied to describe the electronic structure of the system. Notice that the average pair correlation functions of protons $g(\mathbf{R})$ found in both works are not too different from one another. These functions have two maxima at relatively low temperatures and pressures corresponding to the onset of metallization. One maximum is related to the shorter intramolecular distance while the other corresponds to the longer intermolecular one. The maxima are smoothed out as temperature increases, the smoothing being faster in the calculation [89] done with the Car–Parrinello method. However, the main argument of Ref. [89] that favors the inadequacy of considering the hydrogen structure near the metallization transition as 'molecular' is related to temporal processes rather than to the shape of the average pair correlation function $g(\mathbf{R})$. The average time interval was determined within which the distance between two particular protons remained corresponding to the intramolecular maximum of $g(\mathbf{R})$. On the threshold of metallization, this lifetime of a 'molecule' was found to be shorter than the period of intramolecular vibrations. In the opinion of the authors of Ref. [89], there is no reason to speak of the existence of molecules in this case. In fact, short-lived clusters of two protons exist in the system, short-lived clusters of a larger number of protons also being possible. Undoubtedly, this problem calls for extended consideration.

In what follows, we will briefly consider a phase transition due to the molecule dissociation that has been rather rarely discussed in recent years. This problem was studied very actively in the 70s and 80s [4, 26, 50, 90–92]. It was considered most comprehensively by Kagan's group [4, 90] with the use of perturbation theory to fourth order in the electron-proton interaction. At $T = 0$, the energy of the metallic phase depends on the density determined by a dimensionless parameter r_s, as well as on the parameters γ_s characterizing the shape of the unit cell. The electron energy can be developed as a series in the electron-proton interaction:

$$E_{el} = E^{(0)} + E^{(2)} + E^{(3)} + \dots\,, \tag{34}$$

where

$$E^{(n)} = \Omega \sum_{\mathbf{K}_1,\dots,\mathbf{K}_n} \Gamma^{(n)}(\mathbf{K}_1,\dots,\mathbf{K}_n) V(\mathbf{K}_1)\cdot\dots\cdot V(\mathbf{K}_n) \times \Delta(\mathbf{K}_1 + \dots + \mathbf{K}_n)\,. \tag{35}$$

Here $V(\mathbf{k})$ is the electron-ion potential

$$V(\mathbf{k}) = -\frac{4\pi e^2}{k^2 \Omega_0} S(\mathbf{k})\,, \tag{36}$$

$\mathbf{K}_1,\dots,\mathbf{K}_n$ is a vector of the reciprocal lattice, $S(\mathbf{k})$ is the structure factor, $\Delta(\mathbf{K}_1 + \dots + \mathbf{K}_n)$ is the Dirac delta function. A multi-pole function $\Gamma^{(n)}(\mathbf{K}_1,\dots,\mathbf{K}_n)$ is the ordinary linear susceptibility of homogeneous electron gas at $n = 2$, and the nonlinear susceptibility at $n \geqslant 3$. Expressions for them are given in Ref. [90]. An extended analysis of these multi-pole

functions made with the inclusion of exchange and correlation effects is presented in the book [93]. To calculate the total energy of the crystal, E_{el}, one should add the Coulomb energy of protons together with the zero-point contribution E_{vib} to E_{el}:

$$E_{cr} = E_{el} + \frac{1}{2}\sum_{n,n'} \frac{e^2}{|\mathbf{R}_n - \mathbf{R}_{n'}|} + E_{vib}\,. \tag{37}$$

In Refs [4, 90], the quantity E_{vib} was evaluated in the framework of the harmonic approximation,

$$E_{vib} = \frac{1}{2}\sum_{\mathbf{q},\lambda} \hbar\omega(\mathbf{q},\lambda)\,, \tag{38}$$

and the phonon spectrum was determined within a rather rough approximation based on the use of elastic moduli. The pressure range 100 – 1000 GPa corresponding to the density range

$$1.05 \lesssim r_s \lesssim 1.45 \tag{39}$$

received primary consideration. Without going into the details of the calculations [4, 90], we briefly review their results. First of all, the anisotropic crystal structures with very little difference in cohesive energy are stable and energetically favored in metallic hydrogen, practically over the whole density range defined by Eqn (39). As the density increases, an energy minimum is initially reached that corresponds to the formation of structures with $c/a < 1$, distinct from one another by the longitudinal displacement of atomic chains. However, on further increase in density, the $c/a > 1$ structures with a fixed separation of crystal planes but with different ion arrangements in those planes, become energetically favored. This circumstance allowed the authors' of Refs [4, 90] to conclude that metallic hydrogen has a tendency towards fluid-like behavior in the density range (39) and an IM transition from the molecular phase to a liquid metallic one is possible.

The result obtained in Refs [4, 90] have come under criticism [50, 91, 92], especially concerning the fact that the anisotropic structures are energetically preferred. It was stated [50, 91, 92] that taking into account the anharmonism and Debye – Waller factor would change the structure energies situation and lead to the stabilization of simple isotropic structures like hcp or bcc. So far, the crystal structure of the atomic phase of metallic hydrogen has remained unclear. On the one hand, it was confirmed [31] that anisotropic structures are energetically favored, as was obtained by Kagan et al. On the other hand, a Monte Carlo simulation [94] performed at the density corresponding to $r_s = 1.31$ demonstrated that anisotropic structures are favored only in the limit of a static lattice. According to that calculation, the diamond-like structure is the most stable one if the protonic ZPM is taken into account. It should be noted, however, that neither chain- nor layer-like anisotropic structures were actually studied in that work.

The experimental data related to the IM transition observed, presumably, by the VNIIEF group were thoroughly analysed in Ref. [90]. With the theoretical EOS of metallic hydrogen [90] and the EOS of molecular hydrogen [13] the authors of Ref. [90] concluded that the IM transition had been observed at pressures of the order of 300 GPa. In a subsequent experimental work by the VNIIEF group [23], the EOS parameters for the molecular phase were refined and it was shown that a somewhat different EOS might be used, resulting in an estimated transition pressure of ~ 400 GPa. As we have already noted in Section 2 when discussing the EOS problem (see Fig. 1), it is these parameters which lead to excellent agreement with the EOS [5] measured experimentally to 120 GPa by means of static compression in a diamond-anvil cell.

4. Properties of the metallic phase. Superconductivity

Theoretical research of the properties of the hydrogen metallic phase was carried out very intensively in the late 60s and in the 70s. The cardinal problem considered in most of the publications was the possible existence of a superconducting state with a high critical temperature $T_c \gtrsim 200$ K in metallic hydrogen. It was pointed out in an early publication [6] on this problem that such a high value of T_c is of essential astrophysical interest. As is well known [16], Jupiter, for example, consists mainly of hydrogen. Moreover, it is supposed to have rather a low temperature (100 – 200 K) and an appreciable magnetic field. In this case superconductivity may result in a variety of interesting phenomena related to the interaction of normal and superconducting currents and to temporal changes in the total magnetic field of Jupiter. Before proceeding to an extended consideration of the hydrogen superconducting state and of possible T_c values, we briefly discuss a question that, if answered in the affirmative, might turn superconductivity in metallic hydrogen from a problem of fundamental astrophysical importance to one of practical significance. This is the problem of the possible existence of a metastable phase at $p = 0$ that, as was mentioned in the introduction, was first raised by Kagan's group [8]. To clarify this possibility, a few interrelated tasks formulated clearly in Ref. [8] must be solved:

(1) The determination of the metallic hydrogen energy for varying specific volume for various crystal structures; the determination of the lowest energy state.

(2) The verification of the stability of such a phase, which implies, in particular, that all the phonon frequencies must be real, and the phase should be stable with respect to thermal and, we would add, quantum fluctuations.

(3) The determination of the metastable state lifetime.

The first task, and part of the second one, were considered comprehensively in the work under discussion [8]. The calculations were carried out within perturbation theory to the third order in the electron-proton interaction. The total energy was written in the form (34). The metallic hydrogen density corresponding to zero pressure $p = 0$ can be easily estimated if all the contributions of the electron-proton interaction are neglected:

$$r_s = \frac{1.2}{\alpha^2}\left(\frac{1.5}{\pi\alpha} - \alpha_M\right), \tag{40}$$

here $\alpha = [4/(9\pi)]^2 \approx 0.521$ and α_M is the Madelung constant close to 1.8. This gives an r_s value of about 1.65. It is also easy to demonstrate that the bulk modulus satisfies the inequality

$$K_0 = -V\frac{\partial p}{\partial V} > 0\,, \tag{41}$$

at such densities, which ensures stability with respect to long-wavelength density disturbances.

More recent first-principles total-energy calculations [26, 31, 95] made for metallic hydrogen in the framework of DFT confirmed that there is a minimum on the $E-\rho$ curve just in the density range corresponding to $r_s \sim 1.6-1.8$. Things are much more complicated in determining an energetically preferable crystal structure of atomic metallic hydrogen and the dynamical stability of this structure. All the Bravais lattices, and also the diatomic lattices of particular importance, were thoroughly considered in Ref. [8]. It was found that at $p = 0$ metallic hydrogen has a tendency towards crystallization in highly anisotropic structures which is also characteristic of molecular hydrogen as we have seen in the preceding section. Within the perturbation theory to third order, a trigonal family that is based on the simple hexagonal lattice and produces a trigonal 'threadlike' structure with two-dimensional periodicity was demonstrated to be lower in energy. Moreover, it was shown that in the hydrogen metallic phase, a continuous family formed from the simple hexagonal lattice through the following transformation of its basis, a_{10}, a_{20}, a_{30}, with the use of ξ and η parameters

$$a_1 = a_{10} + \xi a_{30}\,, \quad a_2 = a_{20} + \eta a_{30}\,, \quad a_3 = a_{30}\,. \tag{42}$$

is lower in energy, the energy difference for various structures of the family being not more than 10 K.

Since third-order terms of perturbation theory in the electron-proton interaction were essential for all those calculations, and higher orders were not taken into account, it was natural that the conclusions [8] on the existence of a long-lived crystalline metastable phase of metallic hydrogen were challenged by some authors in their publications. Some of those works [10, 11] have already been mentioned in the introduction. This problem was considered in more detail by Avilov and Iordanskiĭ [96]. They applied an unrestricted Hartree–Fock method, different orbitals being used for different spins. The bcc and simple hexagonal crystal structures were studied. First of all, the bcc structure was demonstrated to have a minimum energy at $r_s = 1.7$ that is very close to the r_s value found within perturbation theory in Ref. [8]. Moreover, this minimum value of energy measured with respect to the free atom energy, is also rather close to that found in Ref. [8]. Avilov and Iordanskiĭ point out [96], however, that with correlations included, the minimum shifts to $r_s = 2.3$ and a sharp decrease in cohesive energy occurs. Furthermore, at densities corresponding to $r_s > 2.1$, the hydrogen atomic phase becomes an antiferromagnet with a gap in the electron excitation spectrum. According to the calculation [96], in the simple hexagonal phase the energy as a function of c/a ratio has no minimum though the energy itself is lower than in bcc. With decreasing density, the system is transformed to practically isolated atomic chains.

Somewhat different results were obtained by Kagan et al. [59] when investigating low-density crystalline atomic hydrogen in the limit of only slightly overlapping electrons from different atoms, i.e. in the same density range that was considered in Ref. [96]. The cause for this divergence is rather difficult to judge with certainty, since the approximations of different kinds as well as two dissimilar calculational methods were used in these two studies. The problem concerning the properties of low-density atomic hydrogen has recently been considered in the framework of DFT in Ref. [97]. The results of this work are very close to those obtained in Refs [59, 96], at least as concerning the determination of densities, which correspond, to the antiferromagnetic transition and to the metallization. According to Ref. [8] and the subsequent work [90], it is not improbable that the metastable phase of metallic hydrogen (at $p = 0$), and even its high-pressure metallic phase (at $p > p_c$), may turn out liquid. This conclusion is obviously suggested by the fact that the energy difference between various structures, $\Delta E \sim 10$ K, is insignificant and small as compared to the zero-point energy. This problem was studied [95] by the Monte Carlo method in the framework of the DFT. It was shown that the phase formed at $r_s < 1.5$ is certainly crystalline, but at $r_s > 1.6$ the formation of a fluid metallic phase is much more plausible.

To date, unfortunately, the properties of the metallic hydrogen metastable phase have not been thoroughly calculated beyond the perturbation theory and with both crystalline fields and exchange-correlation effects properly included. Here, the work by Kagan's group [98] should be mentioned where some arguments were advanced in favor of the application of perturbation theory to the problem of the metallic hydrogen metastable phase. However, the question of whether or not the metastable phase exists, still remains to be answered in full. The effect of thermal and quantum fluctuations on the expected lifetime of this phase has not been considered either. Shilov and Ivanov [99, 100] calculated the time of transition from a metastable molecular phase to a metallic one at $p > p_c$ and demonstrated that related processes are very fast. In our opinion which is coherent with the assumptions [10, 96], the main process that prevents the metallic hydrogen metastable phase from being stabilized is the 'pairing' of atoms with the formation of molecules within the chains available in this phase. This process is somewhat similar to the well-known Peierls' instability in one-dimensional metals. The above-mentioned experimental finding of anomalies in compressed Li is, perhaps, another argument in favor of this assumption. The problem of high-density lithium was considered in a recent work [101] within the DFT approach, and it was demonstrated that at densities corresponding to $r_s \approx 2.1$ (at $p = 0$, $r_s = 3.25$ in lithium) a structure transformation occurs just through the 'pairing' of Li atoms with the formation of molecules, and this results in the *Cmca* structure with semimetallic behavior similar to that of a zero-gap semiconductor. On further compression, a transition occurs to the $Cmc2_1$ structure analogous to the structure expected to exist in molecular hydrogen at $p > 150$ GPa and to be already insulating. In Ref. [101], lithium is predicted to transform again into a monoatomic metallic phase similar to the Cs-IV structure only at $r_s < 1.78$ ($p \approx 310$ GPa)

Going to the problem of high-temperature superconductivity in metallic hydrogen, we note that the possibility of a high T_c in this system stems even from the simplest estimation based on the BCS theory. In this approximation T_c may be written in the following form:

$$T_c = \omega_D \exp\left(-\frac{1}{\lambda - \mu^*}\right). \tag{43}$$

Here ω_D is the characteristic phonon frequency, λ is the constant of electron-phonon coupling, and μ^* is the Coulomb pseudopotential.

Metallic hydrogen differs from the majority of ordinary metals in the following features, which favor high T_c values:

(a) first, owing to the small atomic mass of hydrogen, its characteristic ω_D values are much higher than in other metals and may be as high as ~ 1000 K;

(b) second, since the hydrogen atom has no internal electron shells, the electron-proton interaction is merely the Coulomb potential rather than a significantly weaker crystalline pseudopotential which results in a considerably larger λ constant as compared to alkali metals;

(c) third, because the electron density in metallic hydrogen ($r_s < 1.4$) is higher than in alkali metals, the Coulomb pseudopotential turns out to be rather low as well.

All this results in an estimated T_c of the order of 100–300 K in hydrogen. Actually, similar estimates of ω_D, λ, and μ^* were made in early publications [6, 102] on high-temperature superconductivity in metallic hydrogen. Subsequently, more comprehensive investigations [26, 103–107] of this problem have been performed which will be discussed in what follows.

A standard method for calculating the critical temperature of the superconducting transition is the solution of the linearized Eliashberg equations [108] which can be written in the following form:

$$Z(\omega)\Delta(\omega) = \int_{-\infty}^{+\infty} d\omega' \frac{\mathrm{Re}\,\Delta(\omega')}{\omega'} \int_0^{\infty} d\Omega \alpha^2(\Omega) F(\Omega) \times \left[\frac{f(-\omega') + N(\Omega)}{\omega' + \Omega - \omega} + \frac{f(\omega') + N(\Omega)}{\omega' - \Omega - \omega} \right] - \mu \int_0^{\varepsilon_F} d\omega \frac{\mathrm{Re}\,\Delta(\omega')}{\omega'} \tanh \frac{\omega'}{2\tau_c}, \quad (44)$$

$$\big[1 - Z(\omega)\big]\omega = \int_0^{\infty} d\omega' \int_0^{\infty} d\Omega \alpha^2(\Omega) F(\Omega) \times \left[\frac{f(-\omega') + N(\Omega)}{\omega' + \Omega - \omega} - \frac{f(-\omega') + N(\Omega)}{\omega' + \Omega - \omega} + \frac{f(\omega') + N(\Omega)}{-\omega' + \Omega + \omega} - \frac{f(\omega') + N(\Omega)}{-\omega' + \Omega - \omega} \right]. \quad (45)$$

Here $\Delta(\omega)$ is the frequency-dependent order parameter and $Z(\omega)$ is the renormalization function. The $\Delta(\omega)$ parameter is nonzero only in the superconducting state, while $Z(\omega)$ is nonzero in the normal state as well and characterizes the renormalization of electronic spectrum. In particular, in the normal state the $Z(0)$ function has the form:

$$Z(0) = 1 + \lambda, \quad (46)$$

Functions $f(\omega)$ and $N(\omega)$ represent the Fermi- and Bose-distributions, correspondingly, and μ is the average matrix element of Coulomb electron-electron interaction. The $\alpha^2(\omega)F(\omega)$ function is the spectral density of the electron-phonon interaction which is actually the basic quantity responsible for the value of T_c. This function can be written as an integral of the matrix element of the electron-phonon interaction over the Fermi surface:

$$\alpha^2(\Omega)F(\Omega) = \frac{1}{N(\varepsilon_F)} \int \frac{dS_F}{v_F} \left| g^{\mathbf{q},\lambda}_{\mathbf{k}+\mathbf{q},\mathbf{k}} \right|^2 \delta\big[\Omega - \omega(\mathbf{q},\lambda)\big] \times \delta(\varepsilon_{\mathbf{k}}) \delta(\varepsilon_{\mathbf{k}+\mathbf{q}}). \quad (47)$$

Here $N(\varepsilon_F)$ is the density of states at the Fermi level, $\varepsilon_{\mathbf{k}}$ is the spectrum of electron excitations on the Fermi surface, and $\omega(\mathbf{q},\lambda)$ is the phonon spectrum of metal. In the recent review [109], the feasibility of *ab initio* calculation of this function for metals is thoroughly analysed, and for a large number of simple and transition metals, the results of calculating the spectral densities of electron-phonon interaction are presented, revealing that the shape of the $\alpha^2(\omega)F(\omega)$ function coincides closely with the curve of the phonon state density $F(\omega)$. Incidentally it should be mentioned that for metallic hydrogen, such comprehensive calculations of this function are lacking, and it would be of great interest to make them.

The features of the Eliashberg equations as well as of their solutions are described in many books and reviews, so we shall not consider them in close detail here. As an example a review [110] published in *Physics–Uspekhi* in 1982 may be pointed out. Since that time the situation in this field has remained practically unchanged, at least, for superconductors with a moderate constant of electron-phonon coupling, $\lambda \leqslant 2$, which have no soft phonon modes with frequencies $\omega < T_c$. Metallic hydrogen is most likely to fall into this category of metals. It was demonstrated in the review [110] in particular that the critical temperature T_c determined by solving the Eliashberg equations (44), (45) is approximated rather well by an analytical expression of the following form:

$$T_c = \frac{\omega_{\log}}{1.43} \exp\left(\frac{1 + \lambda}{\lambda - \mu^*} \right). \quad (48)$$

Here $\omega_{\log}$ is defined as

$$\omega_{\log} = \frac{2}{\lambda} \int_0^{\infty} d\Omega \frac{\alpha^2(\Omega)F(\Omega)}{\Omega} \ln \Omega, \quad (49)$$

and the Coulomb pseudopotential μ^* is expressed through μ as

$$\mu^* = \frac{\mu}{1 + \mu \ln(\varepsilon_F/\omega_{\log})}. \quad (50)$$

Equation (48) is in good agreement with the McMillan phenomenological formula [111] widely used for these purposes. Thus, the task of T_c calculation, or at least of its reliable estimation, is reduced to the evaluation of such quantities as $\omega_{\log}$, λ, and μ. Actually, this very task was considered in most of the publications devoted to the high-temperature superconductivity in metallic hydrogen (see, for example, Refs [6, 102, 103, 105–107]).

A simple estimate for $\omega_{\log}$ may be obtained by calculating the average phonon frequency. As pointed out already, rather high phonon frequencies may occur in hydrogen because of small proton mass. The plasma frequency of protons responsible for the renormalization of phonon frequencies can be written in the form

$$\omega_{pl} = \left(\frac{4\pi n e^2}{M_p} \right)^{1/2} \approx \frac{1.04}{r_s^{3/2}} \text{ eV}. \quad (51)$$

Phonon frequencies of metals may be somewhat arbitrarily written as

$$\omega^2(\mathbf{q},\lambda) = \omega_{pl}^2 - \omega_{el}^2, \quad (52)$$

where ω_{el}^2 is the electron contribution to the phonon frequency that is expressed in the harmonic approximation through the matrix element of the electron-ion interaction and through the electron susceptibility [112]. In many metals, the electron contribution lowers the average phonon frequen-

cies as against the value of $\omega_{\rm pl}$. The calculations [91, 92] demonstrate that metallic hydrogen is not an exception in this respect, and its average phonon frequencies do not exceed 20–40% of $\omega_{\rm pl}$. Nevertheless, in view of the high $\omega_{\rm pl}$ values, the average phonon frequencies turn out to be of the order of 400–600 K.

Calculating (or at least estimating) the spectral density $\alpha^2(\omega)F(\omega)$ or even the constant of electron-phonon coupling presents more severe difficulties. Such estimates produce a quite considerable spread in the values of the coupling constant λ. A simple estimate with the use of a quasi-isotropic model was reported by Ashcroft in Ref. [6] where the assumption of the possible high-temperature superconductivity of metallic hydrogen was advanced, in fact, for the first time, but turned out to be, actually, too pessimistic. In Ref. [6], a value of $\lambda \approx 0.3$ was obtained, that is too small to favor high $T_{\rm c}$. Curiously enough, approximately the same λ value was reported by one of the present authors in a recent article [107] where more comprehensive calculations were performed within perturbation theory in the electron-proton interaction. More optimistic estimates of λ were obtained in Ref. [102] also with the use of perturbation theory.

Considerably larger values of the coupling constant λ result from *ab initio* electronic-band structure calculations of metallic hydrogen [26, 103, 105, 106]. In the above-cited paper by McMillan [111] λ was expressed in a very simple form:

$$\lambda = \frac{N(\varepsilon_{\rm F})\langle I^2\rangle}{M\langle\omega^2\rangle}\,. \tag{53}$$

Here $N(\varepsilon_{\rm F})\langle I^2\rangle$ may be expressed through the phases δ_l of scattering of electrons by ions (protons) which are directly obtained in band structure calculations:

$$N(\varepsilon_{\rm F})\langle I^2\rangle = \frac{2\varepsilon_{\rm F}}{\pi^2 N(\varepsilon_{\rm F})}\sum_l (l+1)\sin^2(\delta_l-\delta_{l+1}) \times \frac{N_l(\varepsilon_{\rm F})}{N_l^0(\varepsilon_{\rm F})}\,\frac{N_{l+1}(\varepsilon_{\rm F})}{N_{l+1}^0(\varepsilon_{\rm F})}\,. \tag{54}$$

In this case, the Debye frequency found by Caron [91] in the quasiharmonic approximation is used:

$$\omega_{\rm D} = \frac{1.04}{r_{\rm s}^{3/2}} - \frac{0.52}{r_{\rm s}^{1/2}} + 0.018 r_{\rm s}^{1/2}\,. \tag{55}$$

In this expression, the second term is the above-discussed decrease in phonon frequencies as against the $\omega_{\rm pl}$ due to the electron contribution. In the density range corresponding to $1 \leqslant \lambda \leqslant 2$, the coupling constant λ obtained by this method takes the values of $1 < r_{\rm s} < 2$ [26]. Values of about the same order were obtained in Refs [103, 105], the calculated $T_{\rm c}$ values falling over the broad range, $T_{\rm c} \sim 80-250$ K.

Here, the study by Gupta and Sinha [104] based also on the band structure calculation should be mentioned. In all the previous investigations, the bare Coulomb potential was used as an electron-proton potential. It is because of the weakness of the electron-ion pseudopotential that the coupling constant λ in alkali metals is rather small. Since hydrogen has no internal electron shells, there is seemingly no reason to replace the Coulomb potential by a pseudopotential. However, as suggested by Gupta and Sinha [104], with the nonadiabaticity properly included in the electron-phonon interaction, one should take into account that in the vicinity of the proton, the electron wave function is rigidly displaced together with the proton and hence is not involved in the electron-phonon interaction. The estimates [104] made on this basis, demonstrated that the problem reduces again to the replacement of the Coulomb potential by a pseudopotential with the resulting decrease of the coupling constant λ to values of ~ 0.2.

The question of the actual constant of the electron-phonon coupling in metallic hydrogen and of its $T_{\rm c}$ value still remains unanswered, as do most of the questions concerning high-density hydrogen. One such unresolved problem concerning hydrogen superconductivity is the calculation of the Coulomb potential μ^*. It is commonly accepted that $\mu^* = 0.1$ in hydrogen, as in most other metals. But actually, μ^* may be greater or less than this value. Nevertheless, it should be mentioned that at $\lambda \sim 1$, the exact value of μ^* is not so important.

To complete the discussion of high-temperature superconductivity in metallic hydrogen we would like to call attention to a recent article by Richardson and Ashcroft [113] where they considered nontrivial aspects of this problem which are associated with molecular metallic hydrogen. The point is that the electronic structure of molecular metallic hydrogen cannot be properly described in the one-band approximation. Carriers of opposite signs from different bands occur in the system, as for semimetals. As is demonstrated in Ref. [113], taking into account the interaction of different carriers may substantially change the Coulomb contribution to superconductivity to result in additional pairing of electrons. This very statement of a question is by no means new, it has been actively discussed in the context of the general problem of high-temperature superconductivity [114]. In Ref. [113], these effects were calculated in the case of molecular metallic hydrogen using approximate expressions advanced previously [115] for the electron-hole plasma in semiconductors. It was shown [113] that the $T_{\rm c}$ value turns out to be considerably higher than that obtained with the electron-phonon interaction alone involved and may reach ~ 400 K.

5. Conclusions

Let us summarize in brief the discussion of high-pressure hydrogen presented in this review. First of all, it is necessary to state the progress achieved in recent years in the experimental and theoretical study of the problem. The EOS of the molecular phase has been established with rather a high accuracy to ultrahigh pressures (possibly, to 400 GPa, with the VNIIEF results [13, 23] taken into account). The phase diagram of molecular hydrogen has been studied to pressures of ~ 300 GPa. Its crystal structure is also well known to pressures of at least 50 GPa.

Nevertheless, the hydrogen problem turned out to be extremely complicated, both experimentally and theoretically. Thus, one cardinal question relative to this problem still remains open, namely, the value of the metallization pressure. That substances are difficult to investigate experimentally under high pressure, is to some extent self-evident. It is another matter why the theoretical study of this problem turns out to be equally intricate. In our opinion, this situation is not so trivial. As the results obtained by theoreticians and the discussion presented in this review demonstrate, the point is not that some essential processes occurring in high-density hydrogen are incomprehensible to the theoreticians engaged

in the problem. As hydrogen is compressed, structural transformations of different kinds, changes in electronic structure, and the like, occur as in any other system. High-density hydrogen is complicated to study theoretically because any *ad hoc* models are barely helpful to describe these processes. What is required here is a quantitative and precise calculation of specific properties of a particular substance — hydrogen. Owing to a great number of different structures of nearly the same cohesive energy, and owing to the strong crystal-structure dependence of many hydrogen's properties, the energy gap among them, the corresponding calculations demand heavily both higher accuracy and the taking into account of many factors, including, for example, protonic zero-point motion. The solid state theory turned out to be unprepared to solve this problem in full. This is related to insufficient development of both the theoretical methods for calculating crystal properties and the numerical techniques. While a several-percent error in specific volume or in the total energy of crystal due to, for example, the local-density approximation for exchange-correlation energy is not a severe problem for many other systems, an error of this order is crucial for high-density hydrogen since it leads to an energy difference between different crystal structures of the order of fractions of a percent.

Unfortunately, no consistent approach has been developed thus far to go beyond the local density approximation. Besides, a problem of crucial importance, at least in the case of metallic hydrogen — the inclusion of the electron-phonon interaction in the density functional method — is still unsolved. The problem of high-density solid hydrogen is probably among the first in condensed matter physics whose solution imposes such severe quantitative requirements upon the methods of first-principles calculations. But, this problem is certainly not unique. This is possibly true for the calculation of alkali metals in the range of intermediate pressures where they may transform into insulators, as in the example of Li mentioned in this review. A large and serious work lies ahead with the aim of obtaining higher accuracy of *ab initio* methods and applying these methods for investigating the characteristics of high-density hydrogen and similar systems.

The authors express deep gratitude to V L Ginzburg for his constant attention to this work. The work was supported by the International Science and Technology Center (Project No. 207-98) and in part by the Russian Foundation for Basic Research (Grant No. 99-02-16366).

References

1. Wigner E, Huntington H B *J. Chem. Phys.* **3** 764 (1935)
2. Abrikosov A A *Astron. Zh.* **31** 112 (1954)
3. Ross M *J. Chem. Phys.* **60** 3634 (1974)
4. Brovman E G, Kagan Yu, Kholas A *Zh. Eksp. Teor. Fiz* **62** 1492 (1972) [*Sov. Phys. JETP* **35** 783 (1972)]
5. Mao H K, Hemley R J *Rev. Mod. Phys.* **66** 671 (1994)
6. Ashcroft N W *Phys. Rev. Lett.* **21** 1748 (1968)
7. Oliva J, Ashcroft N W *Phys. Rev. B* **23** 6399 (1981)
8. Brovman E G, Kagan Yu, Kholas A *Zh. Eksp. Teor. Fiz.* **61** 783 (1971) [*Sov. Phys. JETP* **34** 528 (1971)]
9. Ginzburg V L *Usp. Fiz. Nauk* **103** 87 (1971); **169** 419 (1999) [*Sov. Phys. Usp.* **14** 21 (1971); *Phys. Usp.* **42** 353 (1999)]; *O Fizike i Astrofizike* (On Physics and Astrophysics) (Moscow: Byuro Kvantum, 1995) [Translated into English: Key Problems in Physics and Astrophysics (Moscow: Mir, 1978)
10. Iordanskiĭ S V et al. *Pis'ma Zh. Eksp. Teor. Fiz.* **17** 530 (1973) [*JETP Lett.* **17** 353 (1973)]
11. Neece G A, Rodgers F J, Hoover W G *Comput. Phys.* **7** 621 (1971)
12. Narayana C et al. *Nature* (London) **393** 46 (1998)
13. Grigor'ev F V et al. *Pis'ma Zh. Eksp. Teor. Fiz.* **16** 286 (1972) [*JETP Lett.* **16** 185 (1972)]; *Zh. Eksp. Teor. Fiz.* **69** 743 (1975) [*Sov. Phys. JETP* **42** 378 (1975)]
14. Hawke P S et al. *Phys. Rev. Lett.* **41** 994 (1978)
15. Silvera I F *Rev. Mod. Phys.* **52** 393 (1980)
16. Stevenson D J *Ann. Rev. Earth Planet Sci.* **10** 257 (1982)
17. Hennes H, Driessen A, Griessen R *J. Phys. C* **19** 3571 (1986)
18. Glazkov V P et al. *Pis'ma Zh. Eksp. Teor. Fiz.* **47** 661 (1988) [*JETP Lett.* **47** 763 (1988)]
19. Hemley R J et al. *Phys. Rev. B* **42** 6458 (1990)
20. Loubeyre P et al. *Nature* (London) **383** 702 (1996)
21. Mao H K et al. *Science* **239** 1131 (1988)
22. Vinet P et al. *J. Phys. C* **19** 467 (1986)
23. Grigor'ev F V et al. *Zh. Eksp. Teor. Fiz.* **75** 1683 (1978) [*Sov. Phys. JETP* **48** 847 (1978)]
24. Birch E *Geophys. Res.* **57** 227 (1952)
25. Murnaghan F D *Proc. Natl. Acad. Sci. USA* **30** 244 (1944)
26. Min B I, Jansen H J F, Freeman A J *Phys. Rev. B* **33** 6383 (1986)
27. Trubitsyn V P *Fiz. Tver. Tela* **7** 3363 (1965); **8** 862 (1966)
28. Ross M, Ree F H, Young D A *J. Chem. Phys.* **79** 1487 (1983)
29. Petrov Yu V *Zh. Eksp. Teor. Fiz.* **84** 776 (1983) [*Sov. Phys. JETP* **57** 449 (1983)]
30. Ferrante J, Smith J R, Rose J H *Phys. Rev. Lett.* **50** 1385 (1983)
31. Barbee T W et al. *Phys. Rev. Lett.* **62** 1150 (1989)
32. Ceperley D M, Alder B *Phys. Rev. B* **36** 2092 (1987)
33. Natoli V, Martin R M, Ceperley D M *Phys. Rev. Lett.* **74** 1601 (1995)
34. Cui L et al. *Phys. Rev. B* **55** 12253 (1997)
35. Kohn W, Sham L J *Phys. Rev. A* **140** 1133 (1965)
36. Goncharov A F et al. *Phys. Rev. Lett.* **75** 2514 (1995)
37. Hanfland M, Hemley R J, Mao H K *Phys. Rev. Lett.* **70** 3760 (1993)
38. Cui L et al. *Phys. Rev. Lett.* **72** 3048 (1994)
39. Mazin I I et al. *Phys. Rev. Lett.* **78** 1066 (1997)
40. Kohanoff J et al. *Phys. Rev. Lett.* **78** 2783 (1997)
41. Edwards B, Ashcroft N W *Nature* (London) **388** 652 (1997)
42. Nagao K, Takezava T, Nagara H *Phys. Rev. B* **59** 13741 (1999)
43. Kaxiras E, Broughton J B, Hemley R J *Phys. Rev. Lett.* **67** 1138 (1991)
44. Nagara H, Nakamura T *Phys. Rev. Lett.* **68** 2468 (1992)
45. Nagao K, Nagara H, Matsubara S *Phys. Rev. B* **56** 2295 (1997)
46. Hohl D et al. *Phys. Rev. Lett.* **71** 541 (1993)
47. Biermann S, Hohl D, Marx D *Solid State Commun.* **108** 337 (1998)
48. Surh M P et al. *Phys. Rev. B* **55** 11330 (1997)
49. Ziman J M "The Calculation of Bloch Functions", in *Solid State Physics* Vol. 26 (Eds H Ehrenreich, F Zeitz, D Turnbull) (New York: Acad. Press, 1971) [Translated into Russian: *Vychislenie Blokhovskikh Funkciĭ* (Moscow: Mir, 1973)]
50. Straus D, Ashcroft N W *Phys. Rev. Lett.* **38** 415 (1977)
51. Edwards B, Ashcroft N W, Lenosky T *Europhys. Lett.* **34** 519 (1996)
52. Surh M P, Barbee T W, Mailhot C *Phys. Rev. Lett.* **70** 4090 (1993)
53. Car R, Parrinello M *Phys. Rev. Lett.* **55** 2471 (1985)
54. Marx D, Parrinello M *Z. Phys. B* **95** 1439 (1994)
55. Tuckerman M E et al. *J. Chem. Phys.* **104** 5579 (1996)
56. Kitaigorodskii A I, Mirskaya K V *Kristallogr.* **10** 121 (1965)
57. Souza I, Martin R M *Phys. Rev. Lett.* **81** 4452 (1998)
58. Baranowski B *Polish J. Chem.* **69** 981 (1995)
59. Kagan Yu, Maksimov L A, Trenin A E *Zh. Eksp. Teor. Fiz.* **75** 693 (1978) [*Sov. Phys. JETP* **48** 871 (1978)]
60. King-Smith R D, Vanderbilt D *Phys. Rev. B* **47** 1651 (1993)
61. *Theory of Inhomogeneous Electron Gas* (Eds S Lundqvist, N H March) (New York: Plenum, 1983) [Translated into Russian: *Teoriya Neodnorodnogo Elektronnogo Gaza* (Eds D A Kirzhnits, E G Maksimov) (Moscow: Mir, 1987)]
62. Struzhkin V V, Hemley R J, Mao H K, in *Abstr. Centenn. Meet. Amer. Phys. Soc., March 1999*, UC30.01; Mori Y, Ruoff A L *ibid.*, UC30.02; Neaton J B, Ashcroft N W *ibid.*, YC10.01
63. Vereshchagin L F, Yakovlev E N, Timofeev Yu A *Pis'ma Zh. Eksp. Teor. Fiz.* **21** 190 (1975) [*JETP Lett.* **21** 85 (1975)]
64. Kawai N, Togaya M, Mishima O *Proc. Jpn. Acad. Sci.* **51** 630 (1975)
65. Yakovlev E N et al. *Pis'ma Zh. Eksp. Teor. Fiz.* **28** 369 (1978) [*JETP Lett.* **28** 340 (1978)]
66. Struzhkin V V et al. *Nature* (London) **380** 382 (1997)
67. Kometani S et al. *J. Phys. Soc. Jpn.* **66** 2564 (1997)

68. Sakharov A D *Usp. Fiz. Nauk* **88** 725 (1966) [*Sov. Phys. Usp.* **9** 294 (1966)]
69. Nellis W J, Weir S T, Mitchell A C *Phys. Rev. Lett.* **76** 1860 (1996); *Phys. Rev. B* **59** 3434 (1999)
70. Friedli C, Ashcroft N W *Phys. Rev. B* **16** 662 (1977)
71. Ramaker D E, Kumar L, Harris F E *Phys. Rev. Lett.* **34** 812 (1975)
72. Balchan A S, Drickamer H G *J. Chem. Phys.* **34** 1948 (1961)
73. Mazin I I, Cohen R E *Phys. Rev. B* **52** R8597 (1995)
74. Herzfeld K F *Phys. Rev.* **29** 701 (1927)
75. Perdew J P, Levy M *Phys. Rev. Lett.* **51** 1884 (1983)
76. Sham L J, Schlüter M *Phys. Rev. Lett.* **51** 1888 (1983)
77. Jones R O, Gunnarson O *Rev. Mod. Phys.* **61** 689 (1989)
78. Maksimov E G et al. *J. Phys.: Condens. Matter* **1** 2493 (1989)
79. Hedin L *Phys. Rev. A* **139** 796 (1965)
80. Godby R W, Schlüter M, Sham L J *Phys. Rev. B* **37** 10159 (1988)
81. Pickett W E, Wang C S *Phys. Rev. B* **30** 4719 (1984)
82. Pickett W E *Comm. Solid State Phys.* **12** 1 (1985)
83. Chacham H, Zhu X, Louie S G *Phys. Rev. B* **46** 6638 (1992)
84. Holm B *Phys. Rev. Lett.* **83** 788 (1999)
85. Allen P B, Heine V *J. Phys. C* **9** 2305 (1976)
86. Allen P B, Cardona M *Phys. Rev. B* **23** 1495 (1981)
87. Mott N F *Metal–Insulator Transitions* (London: Taylor and Francis, 1974) [Translated into Russian (Moscow: Nauka, 1979)]
88. Lenosky T J et al. *Phys. Rev. B* **55** R11907 (1998)
89. Pfaffenzeller O, Hohl D *J. Phys.: Condens. Matter* **9** 11023 (1997)
90. Kagan Yu, Pushkarev V V, Kholas A *Zh. Eksp. Teor. Fiz.* **73** 967 (1977) [*Sov. Phys. JETP* **46** 511 (1977)]
91. Caron L G *Phys. Rev. B* **9** 5025 (1974)
92. Hammerberg J E, Ashcroft N W *Phys. Rev. B* **9** 409 (1974)
93. Gorobchenko V D, Kon V N, Maksimov E G, in *The Dielectric Function of Condensed Matter* (Eds L V Keldysh, D A Kirzhnits, A A Maradudin) (Amsterdam: North-Holland, 1989) p. 87
94. Natoli V, Martin R M, Ceperley D M *Phys. Rev. Lett.* **70** 1952 (1993)
95. Chakraverty S et al. *Phys. Rev. B* **24** 1624 (1981)
96. Avilov V V, Iordanskiĭ S V *Fiz. Tver. Tela* **19** 3516 (1977) [*Sov. J. Solid State* **19** 2054 (1977)]
97. Pfommer B G, Louie S G *Phys. Rev. B* **58** 12680 (1998)
98. Brovman E G et al. *Pis'ma Zh. Eksp. Teor. Fiz.* **18** 160 (1973) [*JETP Lett.* **18** 98 (1973)]
99. Shilov Yu I, Ivanov N R *Fiz. Tver. Tela* **34** 1025 (1992) [*Sov. J. Solid State* **34** 548 (1992)]
100. Shilov Yu I, Ivanov N R *Fiz. Tver. Tela* **34** 1035 (1992) [*Sov. J. Solid State* **34** 1035 (1992)]
101. Neaton J B, Ashcroft N W *Nature* (London) **400** 141 (1999)
102. Schneider T, Stoll E *Physica* **55** 702 (1971)
103. Switendick A C, in *Superconductivity in d- and f-Band Metals* (Ed. D U Douglas) (New York: Plenum, 1976) p. 593
104. Gupta R P, Sinha S K, in *Superconductivity in d- and f-Band Metals* (Ed. D U Douglas) (New York: Plenum, 1976) p. 583
105. Papaconstantopoulos D A, Klein B M *Ferroelectrics* **17** 307 (1977)
106. Barbee T W, Garcia A, Cohen M L *Nature* (London) **340** 369 (1984)
107. Shilov Yu I, Ivanov N R *Fiz. Tver. Tela* **37** 1473 (1994) [*Phys. Solid State* **37** 1473 (1994)]
108. Eliashberg G M *Zh. Eksp. Teor. Fiz.* **38** 966 (1960); **39** 1437 (1960) [*Sov. Phys. JETP* **11** 696 (1960); **12** 1000 (1961)]
109. Maksimov E G, Savrasov D Yu, Savrasov S Yu *Usp. Fiz. Nauk* **167** 337 (1997) [*Phys. Usp.* **40** 317 (1997)]
110. Dolgov O V, Maksimov E G *Usp. Fiz. Nauk* **138** (9) 95 (1982) [*Sov. Phys. Usp.* **25** 688 (1982)]
111. McMillan W L *Phys. Rev.* **167** 331 (1968)
112. Maksimov E G, Savrasov S Yu *Usp. Fiz. Nauk* **165** 773 (1995) [*Phys. Usp.* **38** 737 (1995)]
113. Richardson C F, Ashcroft N W *Phys. Rev. Lett.* **78** 118 (1997)
114. *Problema Vysokotemperaturnoĭ Sverkhprovodimosti* (The Problem of High-Temperature Superconductivity) (Eds V L Ginzburg, D A Kirzhnits) (Moscow: Nauka, 1977) [Translated into English (New York: Consult. Bureau, 1982)]
115. Vignale G, Singwi K S *Phys. Rev. B* **31** 2729 (1985)